3

Analysing Nonlocality in Multiqubit Entangled States under Noisy Conditions and Weak Measurements

3.1 INTRODUCTION

In the previous chapter, we analysed nonlocal correlations in the finally shared two-qubit state under the influence of different noisy channels. We demonstrated the applications of weak measurements and further proposed a two-qubit state for efficient quantum information processing in comparison to other pure and mixed two-qubit entangled states. Similar to two-qubit systems, theoretical as well as experimental characterization of entanglement and nonlocality in multiqubit systems have also been at the center of research to understand foundations of quantum mechanics and quantum information [Home and Selleri, 1991; Khalfin and Tsirelson, 1992; Mermin, 1993; Kwiat *et al.*, 1995; Zeilinger *et al.*, 1997; Zeilinger, 1999; Kwiat *et al.*, 2000; Rungta *et al.*, 2001; Weinfurter and Żukowski, 2001; Batle *et al.*, 2002; Zhao *et al.*, 2004; Thew *et al.*, 2004; Genovese, 2005; Rigolin *et al.*, 2006; Tokunaga *et al.*, 2008; Barreiro *et al.*, 2010; Batle and Casas, 2011; Ma *et al.*, 2011; Lastra *et al.*, 2012; Brandao and Christandl, 2012; Sperling and Vogel, 2013; Brunner *et al.*, 2014; Islam *et al.*, 2015; Batle *et al.*, 2016; Chen *et al.*, 2016; Cianciaruso *et al.*, 2016; Zhao *et al.*, 2016; Hu *et al.*, 2016; Batle *et al.*, 2017; Luo *et al.*, 2017]. Clearly, the analysis of nonlocality not only satisfies the fundamental quest to verify the foundations of quantum mechanics but also leads to secure and optimal quantum information and communication protocols due to the importance of nonlocal correlations [Karlsson and Bourennane, 1998; Shi and Tomita, 2002; Pan *et al.*, 2001a; Agrawal and Pati, 2002; Lee *et al.*, 2002; Wójcik and Grudka, 2003; Zhang and Man, 2005; Agrawal and Pati, 2006; Gordon and Rigolin, 2006; Muralidharan and Panigrahi, 2008; Chamoli and Bhandari, 2009; Das *et al.*, 2014; Herbst *et al.*, 2015; Li *et al.*, 2016b; Singh *et al.*, 2016]. Unlike the pure two-qubit states, where nonlocal correlations are well studied, the characterization of nonlocality in multiqubit systems is much more complex due to the increased complexity of the system [Svetlichny, 1987; Seevinck and Svetlichny, 2002; Collins *et al.*, 2002a,b; Cereceda, 2002; Pan *et al.*, 2003b; Zhao *et al.*, 2003; Eibl *et al.*, 2003, 2004a; Walther *et al.*, 2005a; Lavoie *et al.*, 2009; Ghose *et al.*, 2009, 2010; Ajoy and Rungta, 2010; Bancal *et al.*, 2010; Zhao *et al.*, 2012; Chaves *et al.*, 2012; Tian *et al.*, 2012; Bancal *et al.*, 2013; Barrett *et al.*, 2013a; He and Reid, 2013; Brunner *et al.*, 2014; Fonseca and Parisio, 2015; Paul *et al.*, 2016; de Rosier *et al.*, 2017; Lawrence, 2017]. For example, in case of three-qubit systems one needs to distinguish between bi-separable and genuine tripartite nonlocality; and within the class of genuinely entangled three-qubit states, one needs a way to identify all the entangled states exhibiting genuine quantum correlations [Collins *et al.*, 2002b; Cereceda, 2002; Ghose *et al.*, 2009; Lu *et al.*, 2011b; Zhang *et al.*, 2016]. Precisely, the three-qubit Mermin inequality [Mermin, 1990] is violated by bi-separable as well as genuinely entangled three-qubit states, thus, making it difficult for one to distinguish between bipartite and genuine tripartite nonlocality. Moreover, it is also evident that the Mermin inequality does not identify a set of entangled states in GHZ class for $\tau < 1/2$ or $\tau < 1/4$ [Mermin, 1990; Chi *et al.*, 2010].

In order to confirm the presence of genuine long-range quantum correlations between three and four qubits, one can use the Svetlichny inequality whose violation is a signature of genuine three- or four-qubit correlations [Svetlichny, 1987]. The Svetlichny inequality, however, also fails to identify a set of GHZ states with $\tau<1/2$; nevertheless, the violation of Svetlichny inequality confirms the presence of genuine multiqubit quantum correlations. For four-qubit systems, one can use Scarani-Acin-Schenck-Aspelmeyer (SASA) [Scarani *et al.*, 2005] or Wu-Yeo-Kwek-Oh (WYKO) [Wu *et al.*, 2007] inequalities which are maximally violated by cluster [Briegel and Raussendorf, 2001] and $|\chi\rangle$ type of states [Yeo and Chua, 2006], respectively. Similarly Mermin-Ardehali-Belinskii-Klyshko (MABK) [Mermin, 1990; Ardehali, 1992; Belinskiĭ and Klyshko, 1993] and Werner-Wolf-Zukowski-Brukner (WWZB) [Werner and Wolf, 2001; Żukowski and Brukner, 2002] inequalities are useful for confirming N-qubit nonlocality. Apart from these, there exist several other theoretical and experimental measures based on Bell-type inequalities for estimating nonlocal correlations in multiqubit systems [Chen *et al.*, 2011; Vértesi and Brunner, 2012; Reid *et al.*, 2012; Pramanik and Majumdar, 2012; Lanyon *et al.*, 2014; Chaves *et al.*, 2014; Caban *et al.*, 2015; Sharma *et al.*, 2016; Alsina and Latorre, 2016; Vallins *et al.*, 2017]. In general, entangled resources violating multiqubit Bell-type inequalities are considered to be useful resources for quantum information and computation. As discussed in the previous chapter, these resources, however, suffer from decoherence under real experimental set-ups, and such degradation of nonlocal correlations may lead to non-violation of multiqubit Bell-type inequalities [Zurek, 2003; Carvalho *et al.*, 2004; Hein *et al.*, 2005; Mintert *et al.*, 2005; Bandyopadhyay and Lidar, 2005; Almeida *et al.*, 2007; Liu *et al.*, 2010; Fröwis and Dür, 2011; Mahdian *et al.*, 2012; Ramzan, 2013; Sohbi *et al.*, 2015; Tchoffo *et al.*, 2016]- questioning their usefulness in terms of resources for quantum information and computation. Among several decoherence models proposed [Shor, 1995; Calderbank and Shor, 1996; Steane, 1996; Lidar *et al.*, 1998; Facchi *et al.*, 2004; Sun *et al.*, 2009; Kim *et al.*, 2012; Lu *et al.*, 2011a; Cheong and Lee, 2012; Singh *et al.*, 2018], the one that stands out and is used extensively for protecting entanglement in two-qubit and multiqubit systems, is weak measurement and its reversal operations. For two-qubit systems, we have already demonstrated the pivotal role played by these operations in improving the efficiency of finally shared state in quantum information processing. Hence, the analysis of nonlocal properties in multiqubit systems under real conditions is very important to characterize the complex nature of multiqubit nonlocality and to identify the set of states relevant for quantum information processing.

In this chapter, we readdress the question of three- and four-qubit nonlocality under real experimental or noisy conditions. For this, we consider different classes of three-qubit entangled systems which are shown to be useful for quantum information and computation, e.g., Greenberger-Horne-Zeilinger (GHZ) and W class states [Dür *et al.*, 2000]. The analysis of nonlocal correlations in these systems under real conditions allows us to establish an analytical relation between the maximum value of the Svetlichny operator for a given system, state parameter, noise parameters, and strength of weak measurement and its reversal operations. As examples of noisy channels, we use the interaction between the principal system and the environment through amplitude-damping, phase-damping and depolarization channels. Surprisingly, for generalized GHZ class and amplitude-damping channels, our results indicate that for certain values of weak measurement strengths and range of τ for initially prepared states, the violation of Svetlichny inequality is more if one starts with non-maximally entangled states instead of a maximally entangled GHZ state. Apart from GHZ and W class of states, considering its importance in quantum information processing, we also characterize the nonlocality in W_n type of states [Agrawal and Pati, 2006; Adhikari and Gangopadhyay, 2009; Singh *et al.*, 2016].

Interestingly, for the phase-damping channel, we find that the strength of nonlocal correlation remains independent of the initial entanglement and strength of weak measurement operations. Precisely, after the applications of noise and weak measurement, the expectation value of Svetlichny operator is evaluated to be exactly the same, independent of whether one starts with a maximally or a partially entangled initial state, thereby releasing the constraint to prepare a maximally entangled state to start with. However, for the depolarizing channel, weak measurements and its reversal operations lead to increase in the strength of nonlocal correlations in comparison to the adverse impact of depolarizing noise on quantum correlations. Furthermore, we also describe the nonlocal properties of four-qubit GHZ class states by establishing the analytical relation between maximum expectation value of the four-qubit Svetlichny operator, state parameter, noise parameters and strengths of weak measurement and its reversal operations. We believe that the results obtained in this chapter will be of utmost significance since the states considered here for the analysis of nonlocal correlations are experimentally accessible [Laflamme *et al.*, 1998; Bouwmeester *et al.*, 1999; Pan *et al.*, 2000, 2001b; Eibl *et al.*, 2004b; Dogra *et al.*, 2015; Dong *et al.*, 2016].

3.2 THREE-QUBIT GHZ AND W STATES

Three-qubit states can be classified into two different inequivalent classes, i.e., GHZ class and W class [Dür *et al.*, 2000]. The states of both the classes are shown to be useful for quantum information and computation. The degree of entanglement in the GHZ class is quantified in terms of residual entanglement, i.e., three-tangle (τ) given in Eq. (1.17). As discussed in subsection 1.3.2.(b), the three-tangle, however, fails to capture the genuine entanglement in W class states. Alternately, one can use σ [Emary and Beenakker, 2004] or sum of concurrences of the three reduced bipartite density operators obtained from a W class state as an entanglement measure for W-class states [Dür *et al.*, 2000; Linden *et al.*, 2002]. In this chapter, we use the following two GHZ class states for our analysis, namely the generalized GHZ states

$$|\Psi_g\rangle = \cos\theta\,|000\rangle + \sin\theta\,|111\rangle \tag{3.1}$$

and Slice states [Carteret and Sudbery, 2000]

$$|\Psi_{ms}\rangle = \frac{1}{\sqrt{2}}\{|000\rangle + |11\rangle\{\cos\theta_3\,|0\rangle + \sin\theta_3\,|1\rangle\}\} \tag{3.2}$$

where, θ and θ_3 are state parameters. The maximally entangled GHZ state for $\theta = \pi/4$ or $\theta_3 = \pi/2$, has been used for deterministic transfer of information in many protocols [Karlsson and Bourennane, 1998; Gottesman and Chuang, 1999; Hillery *et al.*, 1999; Raussendorf *et al.*, 2003; Browne and Rudolph, 2005; Lee *et al.*, 2006]. On the similar lines, we further consider two different W class states, namely

$$|\Psi_W\rangle = x\,|001\rangle + y\,|010\rangle + z\,|100\rangle \tag{3.3}$$

where x, y, and z are real, and

$$|\Psi_{W_n}\rangle = \frac{1}{\sqrt{2+2n}}\left[|100\rangle + \sqrt{n}e^{i\delta}\,|010\rangle + \sqrt{n+1}e^{i\zeta}\,|001\rangle\right] \tag{3.4}$$

where n is a positive integer and δ and ζ are relative phases. Unlike the maximally entangled GHZ states, the standard W states cannot be used for deterministic information transfer [Karlsson and Bourennane, 1998; Shi and Tomita, 2002]. On the other hand, $|\Psi_{W_n}\rangle$ states [Agrawal and Pati, 2006] can be used as resources for deterministic teleportation and dense coding. The price one needs to pay for the deterministic information transfer using $|\Psi_{W_n}\rangle$ states is in terms of joint three-qubit measurements. The use of standard single-qubit and two-qubit measurements instead of three-qubit joint measurements leads to significant reduction in the efficiency of $|\Psi_{W_n}\rangle$ states [Adhikari and Gangopadhyay, 2009]. This special class of W states has also been generalized for a case of N-qubits [Singh *et al.*, 2016]. Considering the importance of these states for quantum information, it is essential to characterize nonlocal correlations in these states as well. The study will certainly provide an insight into the usefulness of these resources in real conditions.

3.3 NONLOCALITY IN GHZ CLASS STATES UNDER REAL CONDITIONS

In order to characterize genuine tripartite nonlocality, we use the Svetlichny inequality (SI) [Svetlichny, 1987], S_v, such that

$$S_v(\rho) \equiv |\langle\psi| S_v |\psi\rangle| \leq 4 \tag{3.5}$$

where the Svetlichny operator S_v is given by

$$S_v = A\left(BC + BC' + B'C - B'C'\right) + A'\left(BC - BC' - B'C - B'C'\right) \tag{3.6}$$

and measurements $A = \hat{a}.\sigma_1$, and $A' = \hat{a}'.\sigma_1$ are performed on the first qubit. Here $\hat{a}$, and $\hat{a}'$ are unit vectors, and σ_i's are spin projection operators. The measurements B or B', and C or C' are defined in a similar fashion and are performed on qubits 2 and 3, respectively. The above inequality is satisfied by all separable and bi-separable states, and hence, violation of Svetlichny inequality confirms the presence of genuine tripartite nonlocality in an underlying quantum system.

We now proceed to investigate the effect of decoherence on the violation of Svetlichny inequality for three-qubit GHZ states by establishing an analytical relation between the maximum expectation value of Svetlichny operator, noise parameters and the state parameter. For this,

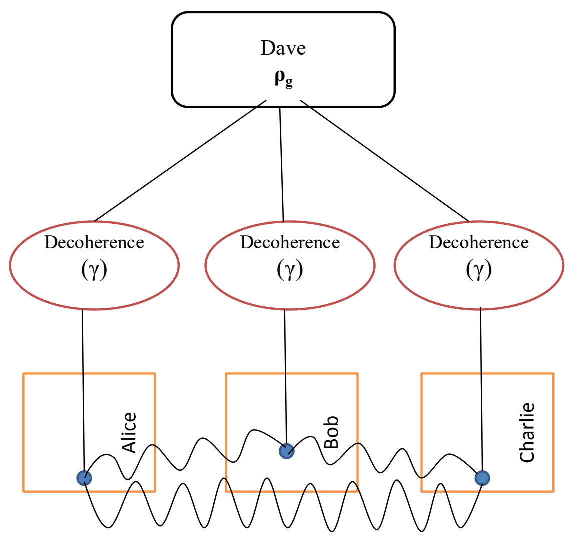

Figure 3.1 : A scenario to analyse the effect of decoherence on maximum expectation value of the Svetlichny operator.

we consider a scenario where Dave prepares a three-qubit pure GHZ state $|\Psi_g\rangle = \cos\theta\,|000\rangle + \sin\theta\,|111\rangle$ and sends one qubit each to Alice, Bob and Charlie through amplitude-damping channels (Figure 3.1) . For the mathematical convenience and simplicity, we consider identical decoherence parameters for all the three channels.

3.3.1 Amplitude-Damping Channel

The single-qubit amplitude-damping channels are represented in Eq. (2.2). Therefore, the three-qubit state of a quantum system after an amplitude-damping noise will evolve as

$$\rho_A^\gamma = \sum_{k,l,m} \left(E_k^1 \otimes E_l^2 \otimes E_m^3\right) \rho \left(E_k^{\dagger 1} \otimes E_l^{\dagger 2} \otimes E_m^{\dagger 3}\right) \tag{3.7}$$

where $k,l,m = (0,1)$. Considering that the shared three-qubit state evolves as $\rho^{\gamma}_{g_A}$, the maximum expectation value for the Svetlichny operator defined in Eq. (3.6) can be obtained by defining

$$\begin{aligned}\hat{a} &= (\sin\theta_a\cos\phi_a, \sin\theta_a\sin\phi_a, \cos\theta_a)\\ \hat{b} &= (\sin\theta_b\cos\phi_b, \sin\theta_b\sin\phi_b, \cos\theta_b)\\ \hat{c} &= (\sin\theta_c\cos\phi_c, \sin\theta_c\sin\phi_c, \cos\theta_c)\end{aligned} \tag{3.8}$$

As earlier, $\hat{a}'$, $\hat{b}'$, and $\hat{c}'$ can be defined in a similar fashion with primes on angles. Moreover, the expression for S_v can be further simplified by defining a pair of mutually orthogonal unit vectors $R = \hat{r}.\sigma_2$ and $R' = \hat{r}'.\sigma_2$ such that $\hat{b} + \hat{b}' = 2\cos\chi.\hat{r}$, and $\hat{b} - \hat{b}' = 2\sin\chi.\hat{r'}$, which leads to

$$\hat{r}.\hat{r'} = \cos\theta_r\cos\theta_{r'} + \sin\theta_r\sin\theta_{r'}\cos(\phi_r - \phi_{r'}) = 0 \tag{3.9}$$

Therefore, Eq. (3.6) can be re-expressed as

$$S_v = 2|\langle ARC\rangle\cos\chi + \langle AR'C'\rangle\sin\chi + \langle A'R'C\rangle\sin\chi - \langle A'RC'\rangle\cos\chi| \tag{3.10}$$

Eq. (3.10) when maximized with respect to χ gives

$$\begin{aligned}S_v &\leq 2\left|\sqrt{\langle ARC\rangle^2 + \langle AR'C'\rangle^2} + \sqrt{\langle A'R'C\rangle^2 + \langle A'RC'\rangle^2}\right|\\ &= M + M'\end{aligned} \tag{3.11}$$

where M and M' are Mermin operators [Mermin, 1990] . Here, we have used the fact that

$$u\cos\theta_1 + v\sin\theta_1 \leq (u^2 + v^2)^{\frac{1}{2}} \tag{3.12}$$

with the equality resulting for $\tan\theta_1 = \frac{v}{u}$. For evaluating the maximum expectation value of $S_v(\rho^{\gamma}_{g_A})$, we first calculate $\langle ARC\rangle$ corresponding to the first term in Eq. (3.11), such that

$$\langle ARC\rangle_{\rho^{\gamma}_{g_A}} = \left[\left(\cos^2\theta + (2\gamma-1)^3\sin^2\theta\right)\cos\theta_a\cos\theta_r\cos\theta_c + \sin 2\theta\,(1-\gamma)^{\frac{3}{2}}\sin\theta_a\sin\theta_r\sin\theta_c\cos(\phi_{arc})\right] \tag{3.13}$$

The expectation value $\langle ARC\rangle_{\rho^{\gamma}_{g_A}}$ can be further maximized with respect to θ_c, i.e.,

$$\langle ARC\rangle_{max} = \left\{\left(\cos^2\theta\ + (2\gamma-1)^3\sin^2\theta\right)^2\cos^2\theta_a\cos^2\theta_r + \sin^2 2\theta(1-\gamma)^3\sin^2\theta_a\sin^2\theta_r\right\}^{\frac{1}{2}} \tag{3.14}$$

where $\cos^2(\phi_{arc}) = \cos^2(\phi_a + \phi_r + \phi_c) = 1$. Similarly $\langle AR'C'\rangle_{max}$ can be given as

$$\langle AR'C'\rangle_{max} = \left\{\left(\cos^2\theta\ + (2\gamma-1)^3\sin^2\theta\right)^2\cos^2\theta_a\cos^2\theta_{r'} + \sin^2 2\theta(1-\gamma)^3\sin^2\theta_a\sin^2\theta_{r'}\right\}^{\frac{1}{2}} \tag{3.15}$$

The maximum values of the operators $\langle A'R'C\rangle$ and $\langle A'RC'\rangle$ can also be defined in a similar way with primes on required angles. Therefore, from Eq. (3.11), we have

$$\begin{aligned}S_v\left(\rho^{\gamma}_{g_A}\right)_{max} &\leq 2\left\{\left(\cos^2\theta\ + (2\gamma-1)^3\sin^2\theta\right)^2\cos^2\theta_a\left(\cos^2\theta_r + \cos^2\theta_{r'}\right)\right.\\ &+ \left.\sin^2 2\theta(1-\gamma)^3\sin^2\theta_a\left(\sin^2\theta_r + \sin^2\theta_{r'}\right)\right\}^{\frac{1}{2}}\\ &+ 2\left\{\left(\cos^2\theta\ + (2\gamma-1)^3\sin^2\theta\right)^2\cos^2\theta_{a'}\left(\cos^2\theta_r + \cos^2\theta_{r'}\right)\right.\\ &+ \left.\sin^2 2\theta(1-\gamma)^3\sin^2\theta_{a'}\left(\sin^2\theta_r + \sin^2\theta_{r'}\right)\right\}^{\frac{1}{2}}\end{aligned} \tag{3.16}$$

In order to further optimize the expectation value of the Svetlichny operator, we use the fact that the maximum of $\cos^2\theta_r + \cos^2\theta_{r'}$ is 1, while the maximum of $\sin^2\theta_r + \sin^2\theta_{r'}$ is 2 [Ghose *et al.*, 2009]. Moreover, we also know that

$$u\cos^2\theta_1 + v\sin^2\theta_1 \le \begin{cases} u, & u \ge v \\ v, & u \le v \end{cases} \tag{3.17}$$

where the first inequality is realized when θ_1=0 or π and the second inequality is realized when $\theta_1=\frac{\pi}{2}$, and hence, Eq. (3.16) can be rewritten as

$$\begin{aligned} & S_v\left(\rho^{\gamma}_{g_A}\right)_{opt} \\ \le\; & 2\left\{\left(\cos^2\theta + (2\gamma-1)^3\sin^2\theta\right)^2\cos^2\theta_a + 2\sin^2 2\theta(1-\gamma)^3\sin^2\theta_a\right\}^{\frac{1}{2}} \\ +\; & \left\{\left(\cos^2\theta + (2\gamma-1)^3\sin^2\theta\right)^2\cos^2\theta_{a'} + 2\sin^2 2\theta(1-\gamma)^3\sin^2\theta_{a'}\right\}^{\frac{1}{2}} \\ \le\; & \begin{cases} 4\left(\cos^2\theta + (2\gamma-1)^3\sin^2\theta\right), & \left(\cos^2\theta + (2\gamma-1)^3\sin^2\theta\right)^2 \ge 2\sin^2 2\theta(1-\gamma)^3 \\ 4\sqrt{2(1-\gamma)^3\sin^2 2\theta}, & \left(\cos^2\theta + (2\gamma-1)^3\sin^2\theta\right)^2 \le 2\sin^2 2\theta(1-\gamma)^3 \end{cases} \end{aligned} \tag{3.18}$$

In case there are no environmental interactions, i.e, Dave sends all the three qubits through perfect channels such that $\gamma = 0$, then by using $\tau(\Psi_g) = \sin^2 2\theta$, the maximum expectation value of Svetlichny operator is

$$S_v\left(\Psi_g\right)_{opt} \le \begin{cases} 4\sqrt{1-\tau(\Psi_g)}, & \tau(\Psi_g) \le \frac{1}{3} \\ 4\sqrt{2\tau(\Psi_g)}, & \tau(\Psi_g) \ge \frac{1}{3} \end{cases} \tag{3.19}$$

The inequality expressed in Eq. (3.19) is exactly the same as the one derived in [Ghose *et al.*, 2009] indicating the maximum expectation value of Svetlichny operator for GGHZ states for transmission through an ideal quantum channel. The analytical result obtained here is in complete agreement

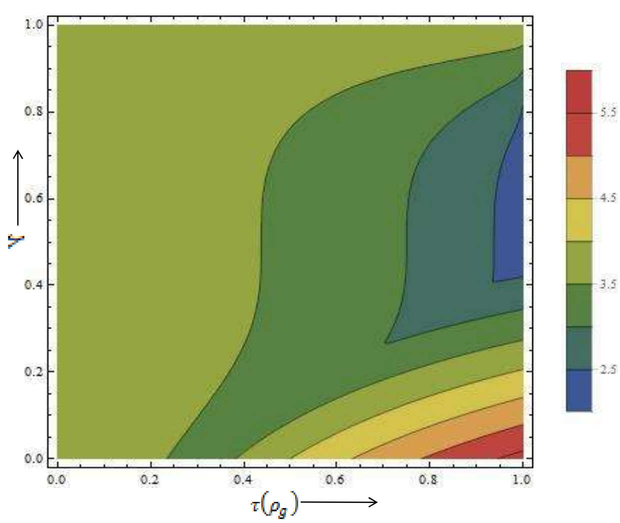

Figure 3.2 : Estimation of maximum value of $S_v(\rho^{\gamma}_{g_A})_{opt}$ vs 3-tangle (τ) of the initial 3-qubit GHZ state with respect to decoherence parameter γ.

with the numerical optimization of the Svetlichny operator for generalized GHZ states under the influence of an amplitude-damping channel. Figure 3.2 clearly describes that the violation of Svetlichny inequality decreases very fast even for small values of noise parameters. Moreover, it also depicts that for noiseless channels and $\tau > \frac{1}{2}$, finally shared state always violates the Svetlichny inequality. The range of violation, however, decreases with increase in the value of decoherence parameter, e.g, see Figure 3.3. Further, in Figure 3.3, A and N stand for analytical and numerical results, respectively, and the same notation will be followed for all the figures hereafter. We now

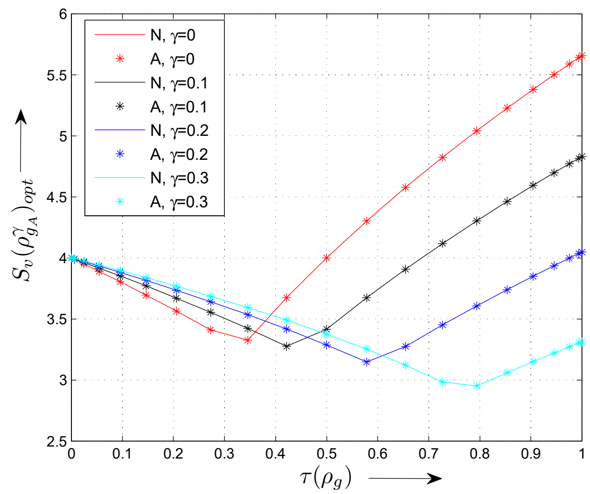

Figure 3.3 : Plot of $S_v(\rho^{\gamma}_{g_A})_{opt}$ with respect to 3-tangle (τ) of the initial 3-qubit GHZ state for four different values of decoherence parameter.

move forward to analyse the effect of weak measurement and quantum measurement reversal operations on nonlocal correlations in presence of the amplitude-damping noise. For this, we

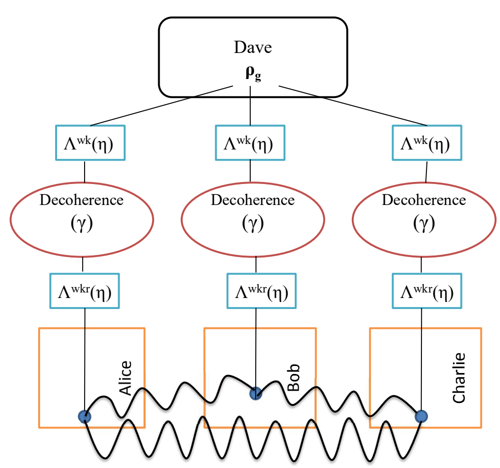

Figure 3.4 : A scenario to analyse the effect of weak measurement and its reversal operations on the existence of genuine tripartite nonlocal correlations.

start with a scenario represented in Figure 3.4 where Dave prepares a three-qubit pure generalized

GHZ state $|\Psi_g\rangle = \cos\theta\,|000\rangle + \sin\theta\,|111\rangle$, and performs weak measurements on each qubit before distributing the qubits through amplitude-damping channels. After receiving the qubits, Alice, Bob and Charlie perform reverse quantum weak measurements on their respective qubits. The form of weak measurement and its reversal operations are described in the previous chapter (Eq. (2.12)). Again for the mathematical convenience and simplicity, we assume same weak measurement strengths for all the channels. Assuming that the strength of weak measurement reversal is optimal, i.e., $\eta_r = \eta + \gamma(1-\eta)$, the expectation value $\langle ARC\rangle$ with respect to the finally shared state is given as

$$\begin{aligned}\langle ARC\rangle_{\rho_{g_A}^{wk}} &= \frac{1}{N_A}\left[\left(\cos^2\theta - (1+\gamma(\eta-1))^3\sin^2\theta\right)\cos\theta_a\cos\theta_r\cos\theta_c\right. \\ &+ \left.\sin 2\theta\cos(\phi_a+\phi_r+\phi_c)\sin\theta_a\sin\theta_r\sin\theta_c\right] \end{aligned} \tag{3.20}$$

where $N_A = \left(\cos^2\theta + (1+\gamma(1-\eta))^3\sin^2\theta\right)$. Similar to the discussion in case of amplitude-damping channels, one can show that the optimum expectation value of the Svetlichny operator for the finally shared state (after implementing the protocol based on weak measurements and quantum measurement reversal) is given as

$$S_v\left(\rho_{g_A}^{wk}\right)_{opt} \leq \begin{cases} \frac{4}{N_A}\left(\cos^2\theta - (1+\gamma(\eta-1))^3\sin^2\theta\right), & \left(\cos^2\theta - (1+\gamma(\eta-1))^3\sin^2\theta\right)^2 \geq 2\sin^2 2\theta \\ \frac{4}{N_A}\sqrt{2\sin^2 2\theta}, & \left(\cos^2\theta - (1+\gamma(\eta-1))^3\sin^2\theta\right)^2 \leq 2\sin^2 2\theta \end{cases} \tag{3.21}$$

For η=1, the expression in Eq. (3.21) will again be the same as for a pure three-qubit GGHZ state [Ghose *et al.*, 2009]. From Figure 3.2 and Figure 3.3, in absence of weak measurement, the

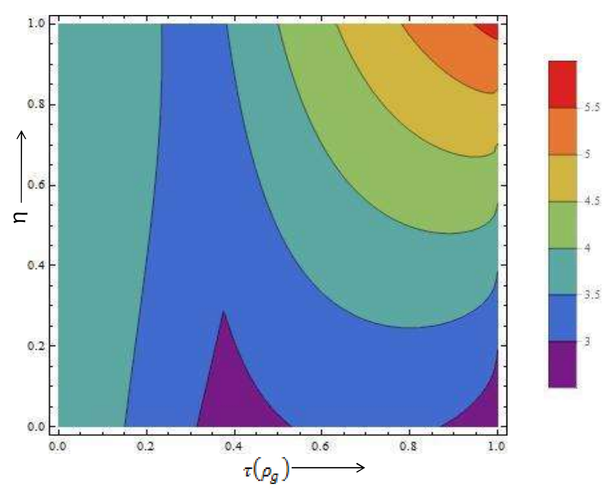

Figure 3.5 : Estimation of maximum value of $S_v(\rho_{g_A}^{wk})_{opt}$ vs 3-tangle (τ) of the initial 3-qubit GHZ state with respect to weak measurement strength parameter η, considering $\gamma = 0.5$.

Svetlichny inequality will not be violated for $\gamma \geq 0.3$ even if the shared initial state is a maximally entangled GHZ state. The effect of weak measurement strengths on the maximum expectation value of Svetlichny operator for a decoherence value of $\gamma = 0.5$ is depicted in Figure 3.5 and Figure

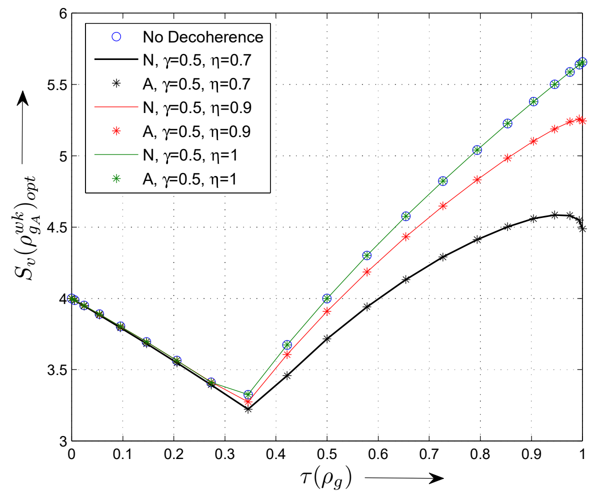

Figure 3.6 : $S_v(\rho_{g_A}^{wk})_{opt}$ with respect to 3-tangle (τ) of initial state for different weak measurement strengths, considering $\gamma = 0.5$.

3.6. Clearly, for a given decoherence parameter the violation of Svetlichny inequality increases with the increase in weak measurement strength. In fact, Figure 3.6 shows that for certain values of weak measurement strengths (except $\eta = 1$) and range of τ of initially prepared states, the violation of Svetlichny inequality is more if one starts with non-maximally entangled pure states instead of a maximally entangled GHZ state. For a maximally entangled initial GHZ state, Figure 3.7 describes

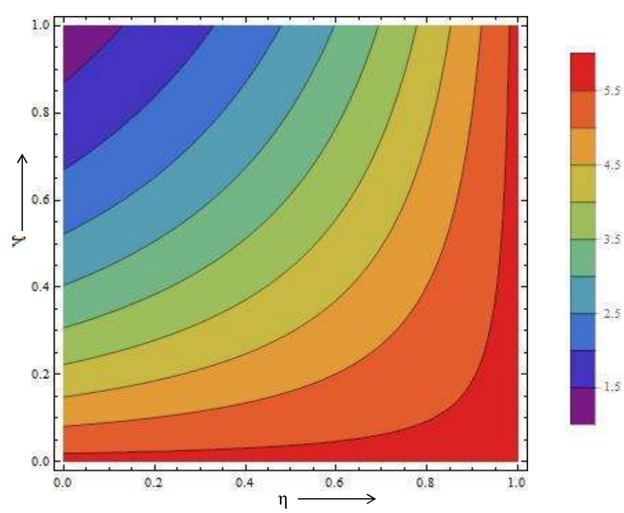

Figure 3.7 : Effect of weak measurement on the maximum expectation value of the Svetlichny operator as a function of noise parameter γ.

the effects of noise parameter and weak measurement strengths on the maximum expectation value of Svetlichny operator. Certainly, the use of weak measurement and quantum measurement reversal is advantageous for enhancing the genuine tripartite nonlocality in the presence of an amplitude-damping noise.

3.3.2 Phase-Damping Channel

We now proceed to analyse the nonlocal correlations in generalized GHZ class under the influence of a phase-damping channel. The single-qubit Kraus operators for phase-damping channels are described in Eq. (2.20). As in the previous cases, for simplicity and mathematical convenience, we consider the qubits to be transmitted through identical decoherence channels, i.e., $\gamma_i = \gamma$, and $i = 1, 2, 3$. Therefore, the initial three-qubit pure state ρ after passing through the phase-damping channels evolves as

$$\rho_P^{\gamma} = \sum_{k,l,m \in (0,1)} \left(E_k^1 \otimes E_l^2 \otimes E_m^3\right) \rho \left(E_k^{\dagger 1} \otimes E_l^{\dagger 2} \otimes E_m^{\dagger 3}\right) \tag{3.22}$$

For our purpose, we consider a scenario where Alice prepares a three-qubit pure GHZ state as represented in Eq. (3.1), and sends second qubit to Bob and third qubit to Charlie through identical phase-damping channels. Therefore, here we consider that Alice performs an identity operation on her qubit 1. Using Eq. (3.22), the three-qubit pure GGHZ state after passing through the phase-damping channel can be represented as

$$\rho_{g_P}^{\gamma} = \begin{pmatrix} f_{11} & 0 & 0 & 0 & 0 & 0 & 0 & f_{18} \\ 0 & 0 & 0 & 0 & 0 & 0 & 0 & 0 \\ 0 & 0 & 0 & 0 & 0 & 0 & 0 & 0 \\ 0 & 0 & 0 & 0 & 0 & 0 & 0 & 0 \\ 0 & 0 & 0 & 0 & 0 & 0 & 0 & 0 \\ 0 & 0 & 0 & 0 & 0 & 0 & 0 & 0 \\ 0 & 0 & 0 & 0 & 0 & 0 & 0 & 0 \\ f_{81} & 0 & 0 & 0 & 0 & 0 & 0 & f_{88} \end{pmatrix} \tag{3.23}$$

where

$$f_{11} = \cos^2\theta \tag{3.24a}$$
$$f_{18} = f_{81} = (1-\gamma)\sin\theta\cos\theta \tag{3.24b}$$
$$f_{88} = \sin^2\theta \tag{3.24c}$$

Considering that the shared three-qubit state evolves as $\rho_{g_P}^{\gamma}$, the maximum value for Svetlichny operator in Eq. (3.6) can be evaluated in a similar way, as in the case of amplitude-damping channels. Hence, for evaluating the maximum expectation value of $S_v(\rho_{g_P}^{\gamma})$, we first calculate the expectation value $\langle ARC \rangle$ in Eq. (3.11) , such that

$$\langle ARC \rangle_{\rho_{g_P}^{\gamma}} = [\cos 2\theta \cos\theta_a \cos\theta_r \cos\theta_c + \sin 2\theta\,(1-\gamma)\sin\theta_a \sin\theta_r \sin\theta_c \cos(\phi_a + \phi_r + \phi_c)] \tag{3.25}$$

The above expectation value $\langle ARC \rangle_{\rho_{g_P}^{\gamma}}$ can be maximized with respect to θ_c, considering $\cos^2(\phi_a + \phi_r + \phi_c) = 1$, i.e.,

$$\langle ARC \rangle_{max} = \left\{\cos^2 2\theta \cos^2\theta_a \cos^2\theta_r + \sin^2 2\theta (1-\gamma)^2 \sin^2\theta_a \sin^2\theta_r\right\}^{\frac{1}{2}} \tag{3.26}$$

Similarly $\langle AR'C' \rangle_{max}$ can be evaluated as

$$\left\langle AR'C' \right\rangle_{max} = \left\{\cos^2 2\theta \cos^2\theta_a \cos^2\theta_{r'} + \sin^2 2\theta (1-\gamma)^2 \sin^2\theta_a \sin^2\theta_{r'}\right\}^{\frac{1}{2}} \tag{3.27}$$

The maximum expectation values of the other two operators $\langle A'R'C \rangle$ and $\langle A'RC' \rangle$ in Eq. (3.11) can be calculated in a similar fashion with primes on required angles. Therefore, we have

$$\begin{aligned} S_v\left(\rho_{g_P}^{\gamma}\right)_{max} &= 2\left\{\cos^2 2\theta \cos^2\theta_a \left(\cos^2\theta_r + \cos^2\theta_{r'}\right) + \sin^2 2\theta (1-\gamma)^2 \sin^2\theta_a \left(\sin^2\theta_r + \sin^2\theta_{r'}\right)\right\}^{\frac{1}{2}} \\ &+ 2\left\{\cos^2 2\theta \cos^2\theta_{a'} \left(\cos^2\theta_r + \cos^2\theta_{r'}\right) + \sin^2 2\theta (1-\gamma)^2 \sin^2\theta_{a'} \left(\sin^2\theta_r + \sin^2\theta_{r'}\right)\right\}^{\frac{1}{2}} \end{aligned} \tag{3.28}$$

The expectation value of $S_v\left(\rho_{gP}^{\gamma}\right)$ can be further optimized using the orthogonality relation between $\vec{r}$ and $\vec{r}'$ so that the maximum value of $\cos^2\theta_r + \cos^2\theta_{r'}$ is 1, and the maximum of $\sin^2\theta_r + \sin^2\theta_{r'}$ is 2, thus

$$S_v\left(\rho_{gP}^{\gamma}\right)_{max} \leq 2\left\{\cos^2 2\theta\cos^2\theta_a + 2\sin^2 2\theta(1-\gamma)^2\sin^2\theta_a\right\}^{\frac{1}{2}} + 2\left\{\cos^2 2\theta\cos^2\theta_{a'} + 2\sin^2 2\theta(1-\gamma)^2\sin^2\theta_{a'}\right\}^{\frac{1}{2}} \quad (3.29)$$

Further, by using Eq. (3.17) to maximize Eq. (3.29) with respect to θ_a and $\theta_{a'}$, and re-expressing $S_v\left(\rho_{gP}^{\gamma}\right)$, we get

$$S_v\left(\rho_{gP}^{\gamma}\right)_{opt} \leq \begin{cases} 4\sqrt{1-\sin^2 2\theta}, & \left(2(1-\gamma)^2+1\right)\sin^2 2\theta \leq 1 \\ 4\sqrt{2(1-\gamma)^2\sin^2 2\theta}, & \left(2(1-\gamma)^2+1\right)\sin^2 2\theta \geq 1 \end{cases} \quad (3.30)$$

Since, the value of three-tangle τ for the generalized GHZ state is $\sin^2 2\theta$, Eq. (3.30) can be rewritten as

$$S_v\left(\rho_{gP}^{\gamma}\right)_{opt} \leq \begin{cases} 4\sqrt{1-\tau(\rho_g)}, & \left(2(1-\gamma)^2+1\right)\tau(\rho_g) \leq 1 \\ 4\sqrt{2(1-\gamma)^2\tau(\rho_g)}, & \left(2(1-\gamma)^2+1\right)\tau(\rho_g) \geq 1 \end{cases} \quad (3.31)$$

If the initially prepared state is a maximally entangled GHZ state, i.e., if $\theta = \frac{\pi}{4}$, then we have

$$S_v\left(\rho_{gP}^{\gamma}\right)_{opt} = 4\sqrt{2}(1-\gamma) \quad (3.32)$$

Figure 3.8 and Figure 3.9 demonstrate that the analytical result obtained here is in complete

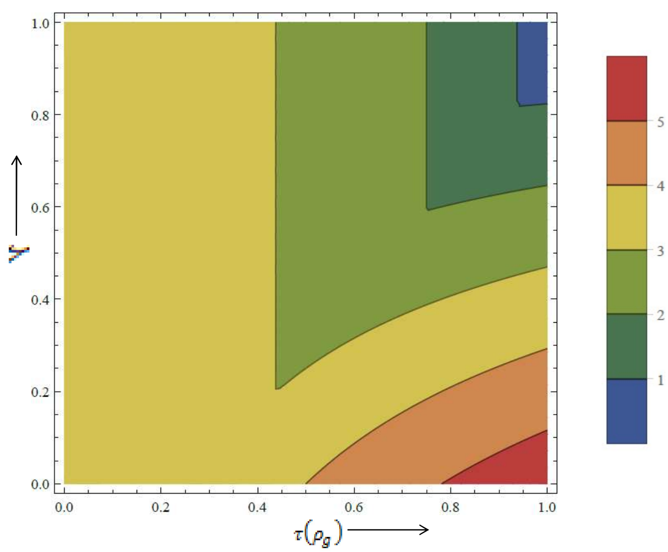

Figure 3.8 : Estimation of maximum value of $S_v(\rho_{gP}^{\gamma})_{opt}$ vs 3-tangle (τ) of the initial 3-qubit GHZ state with respect to decoherence parameter γ.

agreement with the numerical optimization of the Svetlichny operator for generalized GHZ states. It shows that the violation of Svetlichny inequality decreases very fast, even if values of decoherence parameter are very small, i.e., the range of violation decreases rapidly with increase in

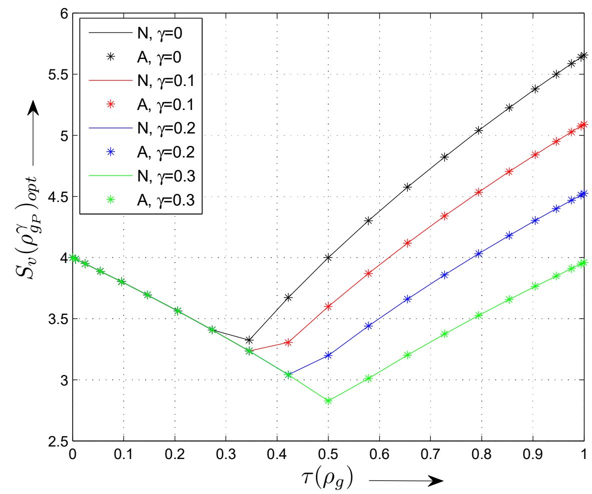

Figure 3.9 : Plot of $S_v(\rho_{gP}^{\gamma})_{opt}$ with respect to 3-tangle (τ) of the initial 3-qubit GHZ state for four different values of decoherence parameter.

the value of decoherence parameter. Moreover, degree of violation of the Svetlichny inequality for the finally shared state is always more if one starts with a maximally entangled initial state rather than starting with a non-maximally entangled initial state under the phase-damping channel. Figure 3.10 shows a plot of noise parameter γ vs Svetlichny operator for three different initial states, i.e., for $\theta = \pi/8$, $\theta = \pi/6$ and $\theta = \pi/4$. Apparently, the range of violation further decreases with the decrease in degree of entanglement of the initial state. Further, if there are no environmental

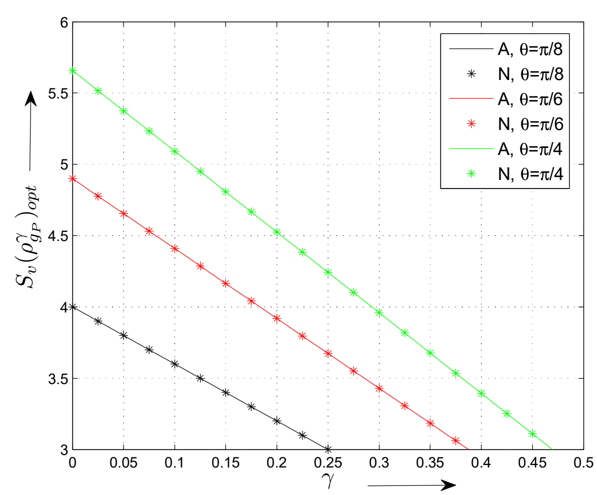

Figure 3.10 : Plot of $S_v(\rho_{gP}^{\gamma})_{opt}$ with respect to decoherence parameter γ for three different input states.

interactions, i.e, if Alice sends qubits to Bob and Charlie through perfect channels, i.e., $\gamma_i = 0$ then the maximum expectation value of Svetlichny operator is

$$S_v(\rho_g) \leq \begin{cases} 4\sqrt{1-\tau(\rho_g)}, & \tau(\rho_g) \leq \frac{1}{3} \\ 4\sqrt{2\tau(\rho_g)}, & \tau(\rho_g) \geq \frac{1}{3} \end{cases} \tag{3.33}$$

The inequality expressed in Eq. (3.33) is the same as Eq. (3.19) for the transmission through an ideal quantum channel.

We now move forward to analyse the effect of weak measurement and its reversal operations to investigate whether the operations suppress the effects of phase-damping noise on quantum correlations or not. For this, we again start with a scenario where Alice prepares a three-qubit pure generalized GHZ state $|\Psi_g\rangle$, and performs weak measurements on qubits 2 and 3 before distributing them through phase-damping channels. After receiving the qubits, Bob and Charlie perform reverse quantum measurements on their respective qubits. Again, we assume same weak measurement strengths for both the qubits for the mathematical convenience and simplicity. Here, we will use weak measurement (Λ^{wk}) and reverse weak measurement (Λ^{wkr}) operators as described in Eq. (2.12).

Therefore, in the given scenario, the three-qubit generalized GHZ state, under the influence of phase-damping noise and weak measurements, evolves as

$$\rho_{gP}^{wk} = \frac{1}{N_P}\begin{pmatrix} g_{11} & 0 & 0 & 0 & 0 & 0 & 0 & g_{18} \\ 0 & 0 & 0 & 0 & 0 & 0 & 0 & 0 \\ 0 & 0 & 0 & 0 & 0 & 0 & 0 & 0 \\ 0 & 0 & 0 & 0 & 0 & 0 & 0 & 0 \\ 0 & 0 & 0 & 0 & 0 & 0 & 0 & 0 \\ 0 & 0 & 0 & 0 & 0 & 0 & 0 & 0 \\ 0 & 0 & 0 & 0 & 0 & 0 & 0 & 0 \\ g_{81} & 0 & 0 & 0 & 0 & 0 & 0 & g_{88} \end{pmatrix} \tag{3.34}$$

where

$$N_P = g_{11} + g_{88} \tag{3.35a}$$
$$g_{11} = (1-\eta_r)^2 \cos^2\theta \tag{3.35b}$$
$$g_{18} = g_{81} = (1-\eta)(1-\eta_r)(1-\gamma)\sin\theta\cos\theta \tag{3.35c}$$
$$g_{88} = (1-\eta)^2 \sin^2\theta \tag{3.35d}$$

Similar to above discussions, we evaluate the expectation value $\langle ARC\rangle$ in Eq. (3.11) with respect to the finally shared state ρ_{gP}^{wk}, such that

$$\begin{aligned} \langle ARC\rangle_{\rho_{gP}^{wk}} &= \frac{1}{N_P}\left[\frac{1}{2}\left\{(\eta-\eta_r)(2-\eta-\eta_r)+\left((1-\eta)^2+(1-\eta_r)^2\right)\cos 2\theta\right\}\cos\theta_a\cos\theta_r\cos\theta_c\right. \\ &+ \left.(1-\gamma)(1-\eta)(1-\eta_r)\sin 2\theta\cos\phi_{arc}\sin\theta_a\sin\theta_r\sin\theta_c\right] \end{aligned} \tag{3.36}$$

where $\cos(\phi_{arc}) = \cos(\phi_a+\phi_r+\phi_c)$. Following the arguments for optimizing the Svetlichny operator in the phase-damping case, one can evaluate the optimum expectation value of the Svetlichny operator for the finally shared state, using weak measurement, and its reversal operations as

$$S_v\left(\rho_{gP}^{wk}\right)_{opt} \leq \begin{cases} \frac{2}{N_P}\left[(\eta-\eta_r)(2-\eta-\eta_r)+\left((1-\eta)^2+(1-\eta_r)^2\right)\sqrt{1-\tau(\rho_g)}\right], \\ \quad \left\{(\eta-\eta_r)(2-\eta-\eta_r)+\left((1-\eta)^2+(1-\eta_r)^2\right)\sqrt{1-\tau(\rho_g)}\right\} \\ \quad \geq \left\{(1-\gamma)(1-\eta)(1-\eta_r)\sqrt{2\tau(\rho_g)}\right\} \\ \frac{4}{N_P}\left[(1-\gamma)(1-\eta)(1-\eta_r)\sqrt{2\tau(\rho_g)}\right], \\ \quad \left\{(\eta-\eta_r)(2-\eta-\eta_r)+\left((1-\eta)^2+(1-\eta_r)^2\right)\sqrt{1-\tau(\rho_g)}\right\} \\ \quad \leq \left\{(1-\gamma)(1-\eta)(1-\eta_r)\sqrt{2\tau(\rho_g)}\right\} \end{cases} \tag{3.37}$$

The optimal weak measurement reversal strength leading to maximum correlations between the qubits is evaluated to be $\eta_r = 1-(1-\eta)\tan\theta$. Therefore, assuming the strength of weak measurement reversal operation to be optimal, the expectation value of Svetlichny operator is re-expressed as

$$S_v\left(\rho_{gP}^{wk}\right)_{opt} = 4\sqrt{2}(1-\gamma) \tag{3.38}$$

Surprisingly, Eq. (3.38) shows that the maximum expectation value of Svetlichny operator for the finally shared tripartite state is independent of the state parameter θ and weak measurement strength η. Furthermore, Eq. (3.38) is the same as Eq. (3.32), and hence for communication protocols affected by phase-damping, one can choose to start with any non-maximally entangled initial three-qubit pure GHZ state instead of a maximally entangled state. The use of weak measurement and its reversal operations, therefore, releases the constraint of preparing a maximally entangled state by optimizing the expectation value of Svetlichny operator to be the same for all θ. A comparison between Figure 3.10 and Figure 3.11 further confirms the importance of use of weak measurement and its reversal operations under phase-damping channels. Interestingly, if we do not consider the optimal strength relation for weak measurement

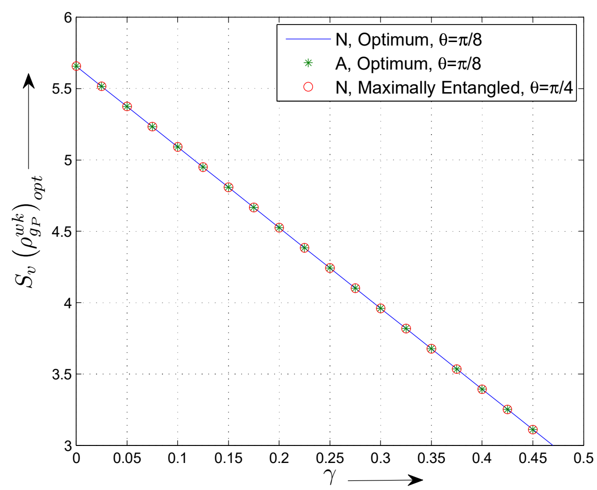

Figure 3.11 : Effect of decoherence on $S_v\left(\rho_{gP}^{wk}\right)_{opt}$ for a maximally and a partially entangled input state under applications of weak measurement.

reversal operation, i.e., $\eta_r = 1-(1-\eta)\tan\theta$ but instead fix its value, say for example $\eta_r = 0.6$, then for a maximally entangled initial state, the extent of violation first increases, attains a maximum value, and then decreases. For example, Figure 3.12 exhibits the behaviour of genuine tripartite nonlocal correlations for a maximally entangled initial state. For small decoherence, the finally shared state attains the maximum violation of $4\sqrt{2}$ at $\eta = 0.6$, which is same as η_r, as the same is also evident from $\eta_r = 1-(1-\eta)\tan\theta$ for $\theta = \pi/4$. Similarly, if we consider $\eta_r = 0.8$ then for the state parameter, $\theta = \frac{\pi}{6}$, Figure 3.13 shows a similar behaviour, i.e., the extent of violation first increases, attains the maximum value, and then decreases. The use of weak measurement and its reversal operations, therefore, can indeed be very useful for protection against the phase-damping decoherence.

3.3.3 Depolarizing Channel

The single-qubit Kraus operators for a depolarizing channel are described in Eq. (2.26). Like the phase-damping case, we again consider identical decoherence parameters for both the

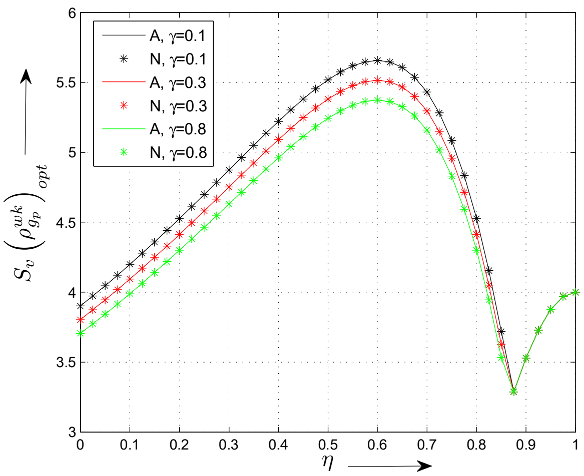

Figure 3.12 : Effect of weak measurement on $S_v\left(\rho_{gP}^{wk}\right)_{opt}$ for a maximally entangled state, considering $\eta_r = 0.6$ at different values of γ.

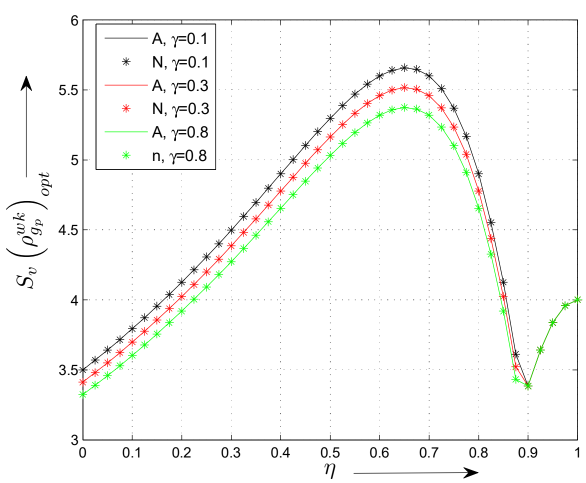

Figure 3.13 : Effect of weak measurement on $S_v\left(\rho_{gP}^{wk}\right)_{opt}$ for a initial state with $\theta = \pi/6$, considering $\eta_r = 0.8$ at different values of γ.

distributed qubits, i.e., $\gamma_1 = \gamma_2 = \gamma$. In this case, the initial three-qubit generalized GHZ state after passing through the depolarizing channel can be given as

$$\rho_{gD}^{\gamma} = \begin{pmatrix} f'_{11} & 0 & 0 & 0 & 0 & 0 & 0 & f'_{18} \\ 0 & f'_{22} & 0 & 0 & 0 & 0 & 0 & 0 \\ 0 & 0 & f'_{33} & 0 & 0 & 0 & 0 & 0 \\ 0 & 0 & 0 & f'_{44} & 0 & 0 & 0 & 0 \\ 0 & 0 & 0 & 0 & f'_{55} & 0 & 0 & 0 \\ 0 & 0 & 0 & 0 & 0 & f'_{66} & 0 & 0 \\ 0 & 0 & 0 & 0 & 0 & 0 & f'_{77} & 0 \\ f'_{81} & 0 & 0 & 0 & 0 & 0 & 0 & f'_{88} \end{pmatrix} \tag{3.39}$$

where

$$f'_{11} = \frac{1}{9}(3-2\gamma)^2\cos^2\theta \tag{3.40a}$$

$$f'_{22} = \frac{4}{9}\gamma^2\sin^2\theta \tag{3.40b}$$

$$f'_{33} = f'_{55} = \frac{2}{9}(3-2\gamma)\,\gamma\cos^2\theta \tag{3.40c}$$

$$f'_{44} = f'_{66} = \frac{2}{9}(3-2\gamma)\,\gamma\sin^2\theta \tag{3.40d}$$

$$f'_{77} = \frac{4}{9}\gamma^2\cos^2\theta \tag{3.40e}$$

$$f'_{88} = \frac{1}{9}(3-2\gamma)^2\sin^2\theta \tag{3.40f}$$

$$f'_{18} = f'_{81} = \frac{1}{9}(3-4\gamma)^2\sin\theta\cos\theta \tag{3.40g}$$

In order to find the maximum expectation value of Svetlichny operator in the evolved three-qubit mixed state $\rho^{\gamma}_{g_D}$, the first term $\langle ARC\rangle$ in Eq. (3.11) can be evaluated as

$$\langle ARC\rangle_{\rho^{\gamma}_{g_D}} = \frac{1}{9}(3-4\gamma)^2\left[\cos 2\theta\cos\theta_a\cos\theta_r\cos\theta_c + \sin 2\theta\sin\theta_a\sin\theta_r\sin\theta_c\cos(\phi_{arc})\right] \tag{3.41}$$

where $\cos(\phi_{arc}) = \cos(\phi_a + \phi_r + \phi_c)$. Similar to the previous cases, we calculate the optimum expectation value of $S_v\left(\rho^{\gamma}_{g_D}\right)$ for the state $\rho^{\gamma}_{g_D}$, shared between Alice, Bob and Charlie, such that

$$S_v\left(\rho^{\gamma}_{g_D}\right)_{opt} \leq \begin{cases} \frac{4}{9}(3-4\gamma)^2\sqrt{1-\sin^2 2\theta}, & \sin^2 2\theta \leq \frac{1}{3} \\ \frac{4}{9}(3-4\gamma)^2\sqrt{2\sin^2 2\theta}, & \sin^2 2\theta \geq \frac{1}{3} \end{cases} \tag{3.42}$$

Since $\tau(\rho_g) = \sin^2 2\theta$, Eq. (3.42) can be rewritten as

$$S_v\left(\rho^{\gamma}_{g_D}\right)_{opt} \leq \begin{cases} \frac{4}{9}(3-4\gamma)^2\sqrt{1-\tau(\rho_g)}, & \tau(\rho_g) \leq \frac{1}{3} \\ \frac{4}{9}(3-4\gamma)^2\sqrt{2\tau(\rho_g)}, & \tau(\rho_g) \geq \frac{1}{3} \end{cases} \tag{3.43}$$

For distribution through perfect channels, i.e., for $\gamma_i = 0$, the maximum expectation value of Svetlichny operator is

$$S_v(\rho_g)_{opt} \leq \begin{cases} 4\sqrt{1-\tau(\rho_g)}, & \tau(\rho_g) \leq \frac{1}{3} \\ 4\sqrt{2\tau(\rho_g)}, & \tau(\rho_g) \geq \frac{1}{3} \end{cases} \tag{3.44}$$

Evidently, the inequality expressed in Eq. (3.44) using the depolarizing noise is the same as Eq. (3.19). Our results, in Figure 3.14, describe the effect of noise parameter γ on the expectation value of Svetlichny operator against the three-tangle of the initially prepared three-qubit generalized GHZ state. One can clearly conclude that the effects of depolarizing noise are much more severe than the effects of amplitude-damping or phase-damping noise- the violation of Svetlichny inequality decreases very fast for small values of noise parameters. Figure 3.15 shows the effects of noise parameter γ on the expectation value of the Svetlichny operator for three different initial states, i.e., for $\theta = \pi/8$, $\theta = \pi/6$ and $\theta = \pi/4$. The range of violation further decreases with decrease in the degree of entanglement of the initial state.

Allied with previous cases, we now evaluate the outcomes of weak measurement and its reversal measurement operations. For depolarizing channel, we define $\sqrt{1-\eta}$ with μ and $\sqrt{1-\eta_r}$ with μ_r in Eq. (2.12) such that the expressions of weak measurement and weak measurement reversal operations are now given as $\Lambda^{wk} = \begin{pmatrix} 1 & 0 \\ 0 & \mu \end{pmatrix}$ and $\Lambda^{wkr} = \begin{pmatrix} \mu_r & 0 \\ 0 & 1 \end{pmatrix}$, respectively [He

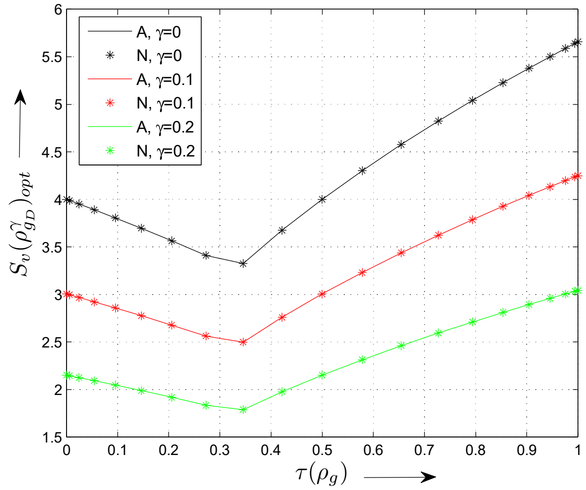

Figure 3.14 : Plot of $S_v(\rho^{\gamma}_{g_D})_{opt}$ with respect to 3-tangle (τ) of the initial 3-qubit GHZ state for three different values of decoherence parameter.

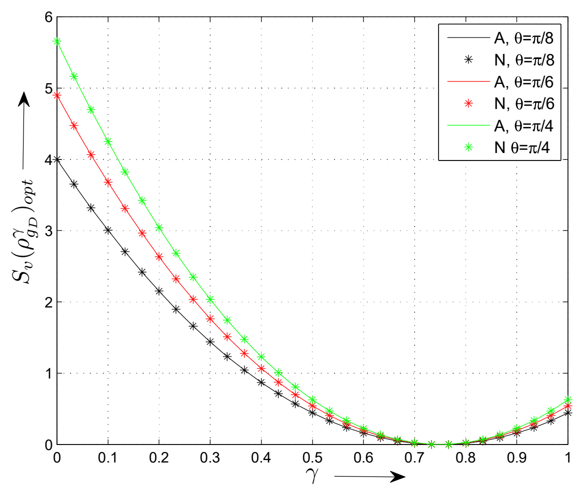

Figure 3.15 : Effect of depolarizing channel on $S_v(\rho^{\gamma}_{g_D})_{opt}$ for three different initial input states.

and Ye, 2015; Singh and Kumar, 2018]. The finally shared state between Alice, Bob and Charlie, therefore, evolves as

$$\rho^{\gamma}_{g_D} = \frac{1}{N_D}\begin{pmatrix} g'_{11} & 0 & 0 & 0 & 0 & 0 & 0 & g'_{18} \\ 0 & g'_{22} & 0 & 0 & 0 & 0 & 0 & 0 \\ 0 & 0 & g'_{33} & 0 & 0 & 0 & 0 & 0 \\ 0 & 0 & 0 & g'_{44} & 0 & 0 & 0 & 0 \\ 0 & 0 & 0 & 0 & g'_{55} & 0 & 0 & 0 \\ 0 & 0 & 0 & 0 & 0 & g'_{66} & 0 & 0 \\ 0 & 0 & 0 & 0 & 0 & 0 & g'_{77} & 0 \\ g'_{81} & 0 & 0 & 0 & 0 & 0 & 0 & g'_{88} \end{pmatrix} \tag{3.45}$$

where

$$N_D = \left(3\mu_r^2 + 2\gamma\left(1-\mu_r^2\right)\right)^2 \cos^2\theta + \left(3-2\gamma\left(1-\mu_r^2\right)\right)^2 \mu^4 \sin^2\theta \tag{3.46a}$$
$$g'_{11} = (3-2\gamma)^2 \mu_r^4 \cos^2\theta \tag{3.46b}$$
$$g'_{22} = 4\gamma^2 \mu_r^4 \mu^4 \sin^2\theta \tag{3.46c}$$
$$g'_{33} = g'_{55} = 2(3-2\gamma)\gamma\mu_r^2 \cos^2\theta \tag{3.46d}$$
$$g'_{44} = g'_{66} = 2(3-2\gamma)\gamma\mu_r^2\mu^4 \sin^2\theta \tag{3.46e}$$
$$g'_{77} = 4\gamma^2 \cos^2\theta \tag{3.46f}$$
$$g'_{88} = (3-2\gamma)^2 \mu^4 \sin^2\theta \tag{3.46g}$$
$$g'_{18} = g'_{81} = 2(3-4\gamma)^2 \mu_r^2 \mu^2 \sin\theta\cos\theta \tag{3.46h}$$

As earlier, for evaluating the maximum expectation value of $S_v(\rho_{gD}^{wk})$, we first evaluate the expectation value, $\langle ARC \rangle$, given in Eq. (3.11), i.e.,

$$\begin{aligned}\langle ARC \rangle_{\rho_{gD}^{wk}} &= \frac{1}{N_D}\Big[\Big\{\left(2\gamma+(2\gamma-3)\mu_r^2\right)^2\cos^2\theta - \left(3-2\gamma\left(1+\mu_r^2\right)\right)^2\mu^4\sin^2\theta\Big\}\cos\theta_a\cos\theta_r\cos\theta_c \\ &+ (3-4\gamma)^2\mu_r^2\mu^2\sin 2\theta\cos^2\phi_{arc}\sin\theta_a\sin\theta_r\sin\theta_c\Big]\end{aligned} \tag{3.47}$$

where $\cos(\phi_{arc}) = \cos(\phi_a + \phi_r + \phi_c)$. One can evaluate the optimum expectation value of the Svetlichny operator for the finally shared state to obtain

$$S_v\left(\rho_{gD}^{wk}\right)_{opt} \leq \begin{cases} \frac{4}{N_D}\Big[\Big\{\left(2\gamma+(2\gamma-3)\mu_r^2\right)^2\cos^2\theta - \left(3-2\gamma\left(1+\mu_r^2\right)\right)^2\mu^4\sin^2\theta\Big\}\Big], \\ \qquad \Big\{\left(2\gamma+(2\gamma-3)\mu_r^2\right)^2\cos^2\theta - \left(3-2\gamma\left(1+\mu_r^2\right)\right)^2\mu^4\sin^2\theta\Big\} \\ \qquad \geq \Big\{(3-4\gamma)^2\mu_r^2\mu^2\sqrt{2\sin^2 2\theta}\Big\} \\ \frac{4}{N_D}\Big[(3-4\gamma)^2\mu_r^2\mu^2\sqrt{2\sin^2 2\theta}\Big], \\ \qquad \Big\{\left(2\gamma+(2\gamma-3)\mu_r^2\right)^2\cos^2\theta - \left(3-2\gamma\left(1+\mu_r^2\right)\right)^2\mu^4\sin^2\theta\Big\} \\ \qquad \leq \Big\{(3-4\gamma)^2\mu_r^2\mu^2\sqrt{2\sin^2 2\theta}\Big\} \end{cases} \tag{3.48}$$

We further evaluate a relationship between weak measurement strength and reverse weak measurement strength for maximizing the amount of correlations in the finally shared state under the influence of a depolarizing channel, such that

$$\mu_r = \left[\frac{\left(4\gamma^2\cos^2\theta + (3-2\gamma)^2\mu^4\sin^2\theta\right)}{\left((3-2\gamma)^2\cos^2\theta + 4\gamma^2\mu^4\sin^2\theta\right)}\right]^{\frac{1}{4}} \tag{3.49}$$

Using above relation, the maximum expectation value of Svetlichny operator can be achieved for $\mu^2 = \cot\theta$, and can be expressed as

$$S_v\left(\rho_{gD}^{wk}\right)_{opt} = \frac{4}{9}\sqrt{2}(3-4\gamma)^2 \tag{3.50}$$

which, in fact, is the same as Eq. (3.43) for a maximally entangled state, i.e, Eq. (3.43) for $\tau(\rho_g) = 1$. Hence, one can deduce that $S_v\left(\rho_{gD}^{wk}\right)_{opt}$ is always greater than $S_v\left(\rho_{gD}^{\gamma}\right)_{opt}$. Furthermore, Figure

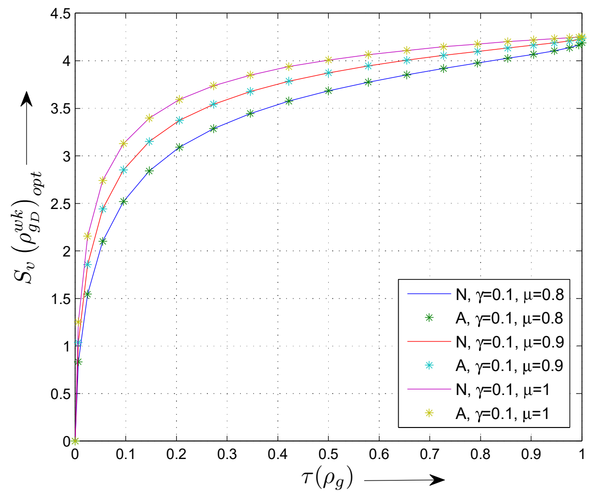

Figure 3.16 : Plot of $S_v(\rho_{gD}^{wk})_{opt}$ with respect to 3-tangle (τ) of the initial three-qubit GHZ state for three different values of weak measurement strength, considering $\gamma = 0.1$.

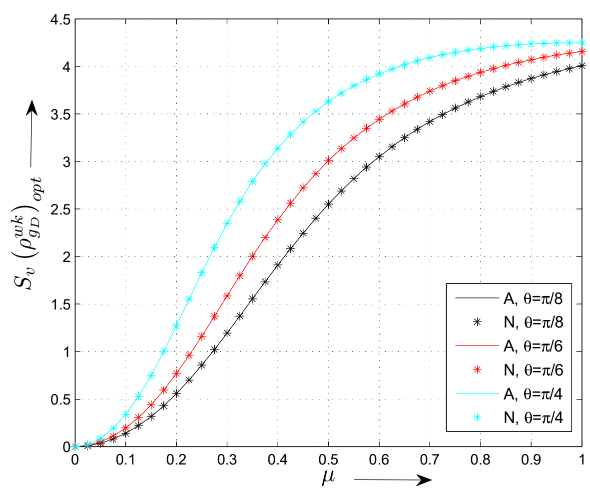

Figure 3.17 : Effect of weak measurement on $S_v\left(\rho_{gD}^{wk}\right)_{opt}$ for three different initial input states, considering $\gamma = 0.1$.

3.16 describes the effect of weak measurement strength on the maximum expectation value of Svetlichny operator against three-tangle of initial state, considering $\gamma = 0.1$ for optimal weak measurement reversal strength. In addition, for optimal weak measurement reversal strength and for initial states with $\theta = \pi/4$, $\theta = \pi/6$, and $\theta = \pi/8$, Figure 3.17 describes the effect of weak measurement strength on the maximum expectation value of Svetlichny operator considering $\gamma = 0.1$. The use of weak measurement and its reversal protocol, therefore, can be useful in protecting the nonlocal correlations against mild depolarizing decoherence.

3.4 ESTIMATION OF NONLOCALITY IN THE GENERALIZED GHZ CLASS STATES

In the previous section, we discussed the nonlocality in generalized GHZ class states under different noisy conditions. Here, we further extend our analysis to describe the effect of amplitude-damping and weak measurement strength on the following class of states,

$$|\Psi_{gs}\rangle = \cos\theta\,|000\rangle + \sin\theta\,|11\rangle\,\{\cos\theta_3\,|0\rangle + \sin\theta_3\,|1\rangle\} \tag{3.51}$$

where θ and θ_3 are state parameters. For $\theta_3 = \pi/2$ and $\theta = \pi/4$, the set of states in Eq. (3.51) correspond to the set of states in Eq. (3.1) and Eq. (3.2), respectively. In this case, we assume that Charlie prepares a three-qubit state as defined in Eq. (3.51), and sends qubit 1 to Alice and qubit 2 to Bob. Before distributing the qubits through amplitude-damping channels, Charlie performs weak measurements on qubits 1 and 2. Similarly, Alice and Bob also perform reverse quantum measurements on their respective qubits once they receive it from Charlie.

Similar to previous cases, in order to find the maximum expectation value of Svetlichny operator in the evolved three-qubit mixed state ρ_{gs}^{wk}, the first term, $\langle ARC\rangle$, in Eq. (3.11) can be expressed as

$$\begin{aligned}\langle ARC\rangle_{\rho_{gs}^{wk}} &= \frac{1}{N'_A}[(\alpha\cos\theta_c+\beta\cos\phi_c\sin\theta_c)\cos\theta_a\cos\theta_r+\sin 2\theta\,(\cos\theta_3\cos\theta_c\cos\phi_{ar}\\ &+ \sin\theta_3\cos\phi_{arc}\sin\theta_c)\sin\theta_a\sin\theta_r]\end{aligned} \tag{3.52}$$

where N'_A=$[(\cos^2\theta+(1+\gamma(1-\eta))^2\sin^2\theta)]$, α=$(\cos^2\theta+(1+\gamma(\eta-1))^2\sin^2\theta\cos 2\theta_3)$, β=$((1+\gamma(\eta-1))^2\sin^2\theta\sin 2\theta_3)$, $\cos\phi_{arc}$=$\cos(\phi_a+\phi_r+\phi_c)$ and $\cos\phi_{ar}$=$\cos(\phi_a+\phi_r)$. Eq. (3.52) can be further maximized using Eq. (3.9) with respect to $(\phi_r-\phi_{r'})$ by considering $\theta_{r'}$, ϕ_r , and $(\phi_r-\phi_{r'})$ to be independent variables. Thus, one can easily deduce that $(\phi_r-\phi_{r'})=0$ and $\theta_r=\frac{\pi}{2}$. Therefore, from Eq. (3.11) the Mermin operator is given as

$$\begin{aligned}M\left(\rho_{gs}^{wk}\right) &= 2\sqrt{\langle ARC\rangle^2+\langle AR'C'\rangle^2}\\ &= \frac{2}{N'_A}\left[\sin^2\theta_a\sin^2 2\theta\left\{(\cos\theta_3\cos\phi_{ar}\cos\theta_c+\sin\theta_3\cos\phi_{arc}\sin\theta_c)^2+(\cos\theta_3\sin\phi_{ar}\cos\theta_{c'}\right.\right.\\ &+ \left.\left.\sin\theta_3\sin\phi_{arc'}\sin\theta_{c'})^2\right\}+\cos^2\theta_a\,(\alpha\cos\theta_{c'}+\beta\cos\phi_{c'}\sin\theta_{c'})^2\right]^{\frac{1}{2}}\end{aligned} \tag{3.53}$$

The sequential optimization of the Mermin operator is summarized below as

$$M\left(\rho_{gs}^{wk}\right)$$

$$\leq \begin{cases}\frac{2}{N'_A}\sin 2\theta\left\{(\cos\theta_3\cos\phi_{ar}\cos\theta_c+\sin\theta_3\cos\phi_{arc}\sin\theta_c)^2+(\cos\theta_3\sin\phi_{ar}\cos\theta_{c'}\right.\\ \left.+\sin\theta_3\sin\phi_{arc'}\sin\theta_{c'})^2\right\}^{\frac{1}{2}}\\ \frac{2}{N'_A}(\alpha\cos\theta_{c'}+\beta\cos\phi_{c'}\sin\theta_{c'})\end{cases} \tag{3.54}$$

$$\leq \begin{cases}\frac{2}{N'_A}\sin 2\theta\left\{\left(\cos^2\theta_3\cos^2\phi_{ar}+\sin^2\theta_3\cos^2\phi_{arc}\right)+\left(\cos^2\theta_3\sin^2\phi_{ar}+\sin^2\theta_3\sin^2\phi_{arc'}\right)\right\}^{\frac{1}{2}}\\ \frac{2}{N'_A}\left(\alpha^2+\beta^2\cos^2\phi_{c'}\right)^{\frac{1}{2}}\end{cases} \tag{3.55}$$

$$\leq \begin{cases}\frac{2}{N'_A}\sin 2\theta\sqrt{1+\sin^2\theta_3}\\ \frac{2}{N'_A}\sqrt{\alpha^2+\beta^2}\end{cases} \tag{3.56}$$

$$\leq \begin{cases}\frac{2}{N'_A}\sin 2\theta\sqrt{1+\sin^2\theta_3}\\ \frac{2}{N'_A}\left\{\left(\cos^2\theta+(1+\gamma(\eta-1))^2\sin^2\theta\right)^2-(1+\gamma(\eta-1))^2\sin^2 2\theta\sin^2\theta_3\right\}^{\frac{1}{2}}\end{cases} \tag{3.57}$$

where we have used the inequalities (3.12) and (3.17). In the above equations, the maximization is performed with respect to $\theta_{r'}$ in Eq. (3.53), θ_a in Eq. (3.54), and θ_c and $\theta_{c'}$ in Eq. (3.55). Furthermore, in Eq. (3.56) we assumed that $\phi_{ar} = 0$, $\phi_{arc} = 0$, and $\phi_{arc'} = \frac{\pi}{2}$. Similarly, the optimized value for operator M' turns out to be the same as in Eq. (3.57) by considering $A \rightarrow A'$ and $C \rightarrow C'$. Moreover, three-tangle and residual concurrence for the states $|\Psi_{gs}\rangle$ are given by $\tau(\rho_{gs}) = \sin^2 2\theta \sin^2\theta_3$ and $C_{12}^2(|\Psi_{gs}\rangle) = \sin^2 2\theta \cos^2\theta_3$, respectively. Therefore, using these expressions for three-tangle and residual concurrence of the input state, the optimum value of Svetlichny operator can be re-expressed as

$$S_v\left(\rho_{gs}^{wk}\right)_{opt} \leq \begin{cases} \frac{4}{N_A'} \sin 2\theta \sqrt{1+\sin^2\theta_3} \\ \frac{4}{N_A'} \left\{ \left(\cos^2\theta + (1+\gamma(\eta-1))^2 \sin^2\theta\right)^2 - (1+\gamma(\eta-1))^2 \sin^2 2\theta \sin^2\theta_3 \right\}^{\frac{1}{2}} \end{cases} \tag{3.58}$$

$$\leq \begin{cases} \frac{4}{N_A'} \sqrt{2\tau + C_{12}^2}, \\ \qquad\qquad \left(2+(1+\gamma(\eta-1))^2\right)\tau + C_{12}^2 \geq \left(\cos^2\theta + (1+\gamma(\eta-1))^2\sin^2\theta\right)^2 \\ \frac{4}{N_A'} \left\{ \left(\cos^2\theta + (1+\gamma(\eta-1))^2 \sin^2\theta\right)^2 - (1+\gamma(\eta-1))^2\tau \right\}^{\frac{1}{2}}, \\ \qquad\qquad \left(2+(1+\gamma(\eta-1))^2\right)\tau + C_{12}^2 \leq \left(\cos^2\theta + (1+\gamma(\eta-1))^2\sin^2\theta\right)^2 \end{cases} \tag{3.59}$$

Clearly, for perfect channels, i.e., for $\gamma = 0$, the maximum expectation value of Svetlichny operator is the same as derived in [Ajoy and Rungta, 2010]. Similarly, for weak measurement strength, $\eta = 1$, the effect of decoherence fully vanishes and the optimum value of Svetlichny operator is again the same as given in [Ajoy and Rungta, 2010]. Figure 3.18 shows the relationship

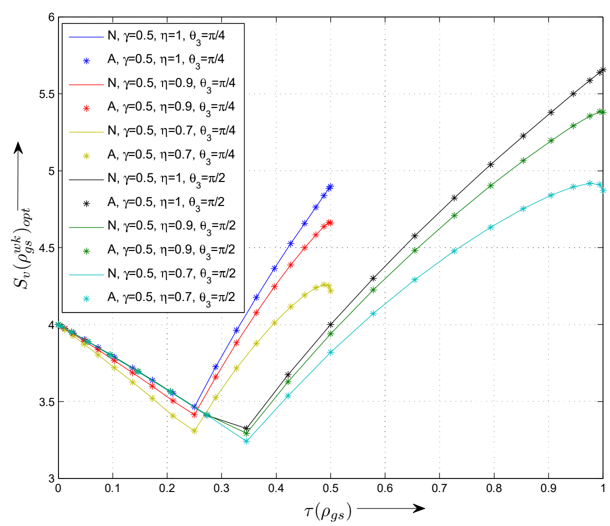

Figure 3.18 : $S_v(\rho_{gs}^{wk})_{opt}$ with respect to 3-tangle (τ) of the initial state for different weak measurement strengths, considering $\gamma = 0.5$ for two different values of $\theta_3 = (\frac{\pi}{4}, \frac{\pi}{2})$.

between $S_v\left(\rho_{gs}^{wk}\right)_{opt}$ and 3-tangle (τ) of the input state, for different values of weak measurement strength considering noise parameter $\gamma = 0.5$, for two different sets of GHZ states, i.e., for $\theta_3 = \frac{\pi}{2}$, and $\theta_3 = \frac{\pi}{4}$. Moreover in Figure 3.19, we show the relation between $S_v\left(\rho_{gs}^{wk}\right)_{opt}$ and 3-tangle

(τ) of the initial input state, i.e., MS state ($\theta = \frac{\pi}{4}$), for different values of weak measurement strength, considering noise parameter $\gamma = 0.5$. Clearly, for $\eta = 1$, the effect of decoherence is fully suppressed as the finally shared state always violates the Svetlichny inequality; and for lower values of weak measurement strength, the finally shared state still violates the Svetlichny inequality for a considerable range of three-tangle of the initial input state.

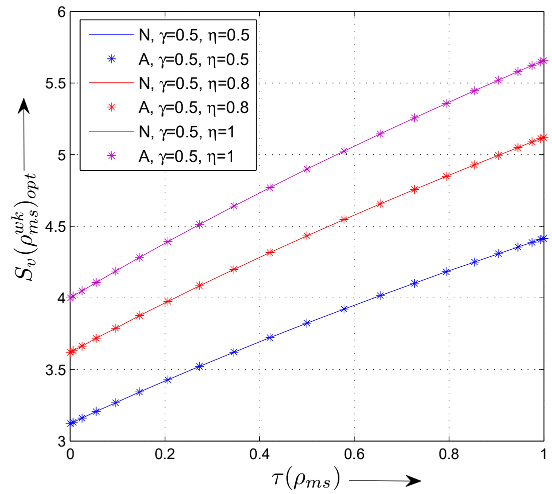

Figure 3.19 : $S_v(\rho_{ms}^{wk})_{opt}$ with respect to 3-tangle (τ) of the initial state for different weak measurement strengths, considering $\gamma = 0.5$ and $\theta = \frac{\pi}{4}$.

We further establish a relation between the maximum expectation value of the Svetlichny operator and negativity [Sabín and García-Alcaine, 2008b] of the finally shared three-qubit mixed state, numerically. For example, Figure 3.20 and Figure 3.21 demonstrate the effect of

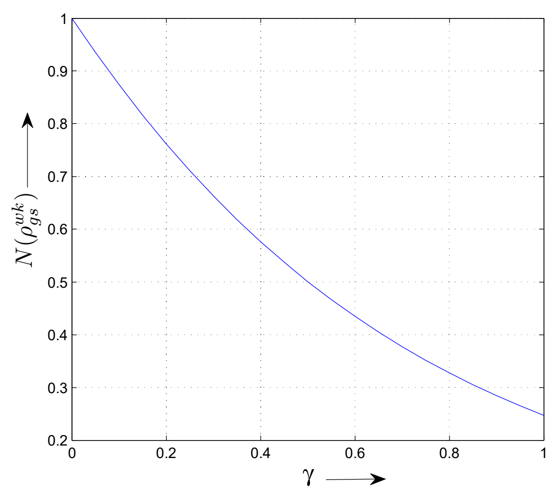

Figure 3.20 : Negativity of the finally shared 3-qubit state as a function of noise parameter γ.

amplitude-damping noise and weak measurement strength, respectively on the negativity of the finally shared state. Lastly, in Figure 3.22, we show the relation between the optimum expectation value of Svetlichny operator and negativity of finally shared state for different values of weak measurement strength, considering $\gamma = 0.5$ and $\theta_3 = \frac{\pi}{2}$.

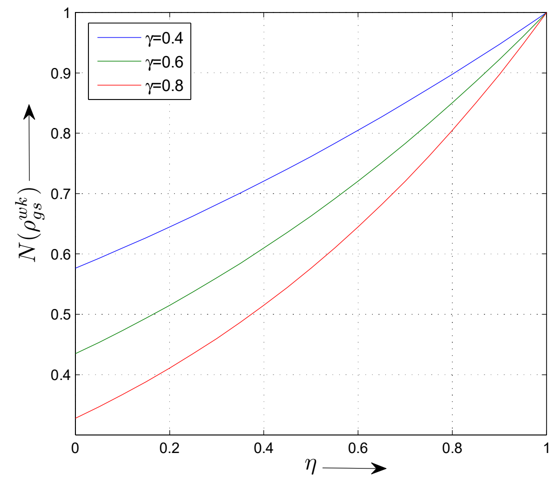

Figure 3.21 : Negativity of the finally shared 3-qubit state as a function of weak measurement strength η at different values of decoherence parameter γ.

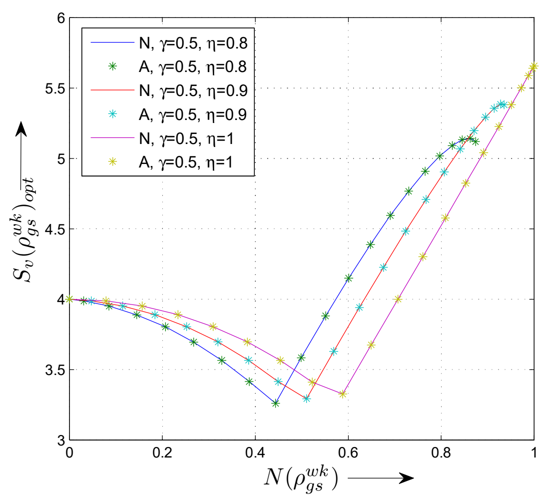

Figure 3.22 : Plot of maximum expectation value of the Svetlichny operator $S_v(\rho_{gs}^{wk})_{opt}$ with respect to Negativity N of the finally shared state for different values of weak measurement strength, considering $\gamma = 0.5$.

3.5 ANALYSIS OF NONLOCAL CORRELATIONS IN THE W CLASS AND W_N-TYPE STATES

We now proceed to analyse another important class of three-qubit states, i.e., W states as represented in Eq. (3.3). Ajoy and Rungta [Ajoy and Rungta, 2010] have shown that the Svetlichny inequality is more suitable to identify the tripartite nonlocality in W class of states- the inequality, though, is violated only when the sum of concurrences of three bipartite reduced states exceeds a certain threshold.

In order to analyse nonlocal correlations in W states in a similar communication scenario as described in the previous section, we first calculate the expectation value of the first term, i.e., $\langle ABC\rangle$ in Eq. (3.6), in the evolved three-qubit state ρ_W^{wk}, such that

$$\begin{aligned}\langle ABC\rangle_{\rho_W^{wk}} &= \cos\theta_b\left(C_{31}\sin\theta_a\sin\theta_c\cos\phi_{ac}-\Delta\cos\theta_a\cos\theta_c\right)\\ &+ \sin\theta_b\left(C_{12}\cos\theta_a\sin\theta_c\cos\phi_{bc}+C_{23}\sin\theta_a\cos\theta_c\cos\phi_{ab}\right)\end{aligned} \tag{3.60}$$

where $\Delta=\frac{(x^2+(1+\gamma(\eta-1))(y^2+z^2))}{(x^2+(1+\gamma(1-\eta))(y^2+z^2))}$, $\cos\phi_{ab}=\cos(\phi_a-\phi_b)$, $C_{12}=\frac{2xy}{(x^2+(1+\gamma(1-\eta))(y^2+z^2))}$, $C_{23}=\frac{2yz}{(x^2+(1+\gamma(1-\eta))(y^2+z^2))}$, and $C_{31}=\frac{2xz}{(x^2+(1+\gamma(1-\eta))(y^2+z^2))}$. For maximizing the value of Svetlichny operator, we first assume $\phi_i=0$ [Ajoy and Rungta, 2010], and then add the first four terms in Eq. (3.6) to get

$$\begin{aligned}\langle M\rangle &= \frac{1}{4}[(-\Delta-C_{12}-C_{23}-C_{31})\{\cos(\theta_a+\theta_b+\theta_{c'})+\cos(\theta_{a'}+\theta_b+\theta_c)+\cos(\theta_a+\theta_{b'}+\theta_c)\\ &- \cos(\theta_{a'}+\theta_{b'}+\theta_{c'})\}\\ &+ (-\Delta+C_{12}-C_{23}+C_{31})\{\cos(\theta_a+\theta_b-\theta_{c'})+\cos(\theta_{a'}+\theta_b-\theta_c)+\cos(\theta_a+\theta_{b'}-\theta_c)\\ &- \cos(\theta_{a'}+\theta_{b'}-\theta_{c'})\}\\ &+ (-\Delta+C_{12}+C_{23}-C_{31})\{\cos(\theta_a-\theta_b+\theta_{c'})+\cos(\theta_{a'}-\theta_b+\theta_c)+\cos(\theta_a-\theta_{b'}+\theta_c)\\ &- \cos(\theta_{a'}-\theta_{b'}+\theta_{c'})\}\\ &+ (-\Delta-C_{12}+C_{23}+C_{31})\{\cos(\theta_a-\theta_b-\theta_{c'})+\cos(\theta_{a'}-\theta_b-\theta_c)+\cos(\theta_a-\theta_{b'}-\theta_c)\\ &- \cos(\theta_{a'}-\theta_{b'}-\theta_{c'})\}]\end{aligned} \tag{3.61}$$

The expression for M' can be written in a similar fashion. For simplicity and mathematical convenience, let us define $\Sigma=\left(\theta'_a+\theta'_b+\theta'_c\right)$, $\Sigma_k=\Sigma-2\theta'_k$, $\tilde{\theta}_k=(\theta_k+\theta_{k'})/2$, and $\theta'_k=(\theta_{k'}-\theta_k)/2$ where $k\in\{a,b,c\}$, such that

$$\begin{aligned}S_v\left(\rho_W^{wk}\right)_{opt} &= \frac{1}{2}\left[(-\Delta-C_{12}-C_{23}-C_{31})\sin\left(\tilde{\theta}_a+\tilde{\theta}_b+\tilde{\theta}_c\right)\left\{K-2\sin\left(\theta'_a-\theta'_b-\theta'_c\right)\right\}\right.\\ &+ (-\Delta+C_{12}-C_{23}+C_{31})\sin\left(\tilde{\theta}_a+\tilde{\theta}_b-\tilde{\theta}_c\right)\left\{K-2\sin\left(\theta'_a-\theta'_b+\theta'_c\right)\right\}\\ &+ (-\Delta+C_{12}+C_{23}-C_{31})\sin\left(\tilde{\theta}_a-\tilde{\theta}_b+\tilde{\theta}_c\right)\left\{K-2\sin\left(\theta'_a+\theta'_b-\theta'_c\right)\right\}\\ &+ \left.(-\Delta-C_{12}+C_{23}+C_{31})\sin\left(\tilde{\theta}_a-\tilde{\theta}_b-\tilde{\theta}_c\right)\left\{K-2\sin\left(\theta'_a+\theta'_b+\theta'_c\right)\right\}\right]\\ &= \Delta\{\sin\Sigma_a+\sin\Sigma_b+\sin\Sigma_c-\sin\Sigma\}+C_{12}\{\sin\Sigma-\sin\Sigma_a+\sin\Sigma_b+\sin\Sigma_c\}\\ &+ C_{23}\{\sin\Sigma+\sin\Sigma_a+\sin\Sigma_b-\sin\Sigma_c\}+C_{31}\{\sin\Sigma+\sin\Sigma_a-\sin\Sigma_b+\sin\Sigma_c\}\end{aligned} \tag{3.62}$$

here the second equality is obtained by considering $\tilde{\theta}_a=\tilde{\theta}_b=\tilde{\theta}_c=\pi/2$. Hence,

$$S_v\left(\rho_W^{wk}\right)_{opt}\equiv 4\left(s_1\Delta+s_2C_{12}+s_3C_{23}+s_4C_{31}\right) \tag{3.63}$$

where

$$K=\left\{\sin\left(\theta'_a+\theta'_b+\theta'_c\right)+\sin\left(\theta'_a-\theta'_b+\theta'_c\right)+\sin\left(\theta'_a+\theta'_b-\theta'_c\right)\sin\left(\theta'_a-\theta'_b-\theta'_c\right)\right\} \tag{3.64}$$

From Eq. (3.63), we can see that the finally shared tripartite entangled states will violate the Svetlichny inequality iff $(s_1\Delta+s_2C_{12}+s_3C_{23}+s_4C_{31})>1$. Clearly, for weak measurement strength $\eta=1$, the effect of decoherence fully vanishes, and a general tripartite entangled W state violates the Svetlichny inequality when $(s_1+s_2C'_{12}+s_3C'_{23}+s_4C'_{31})>1$, where $C'_{12}=2xy$, $C'_{23}=2yz$, and $C'_{31}=2xz$ are the concurrences of the three reduced states of input state $|\Psi_W\rangle$. Moreover, the

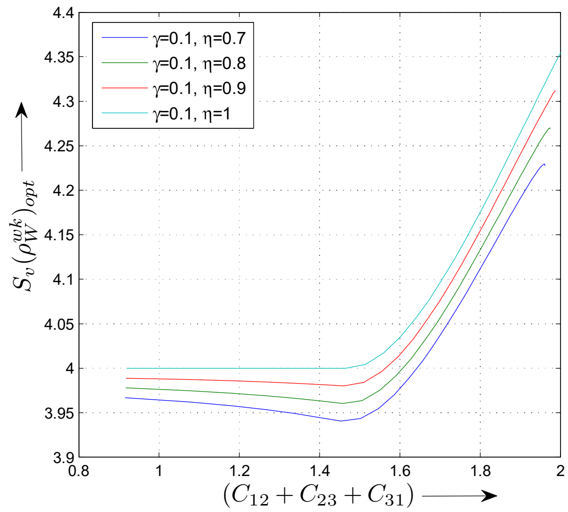

Figure 3.23 : Maximum expectation value of $S_v(\rho_W^{wk})_{opt}$ with respect to the varying sum of concurrences $(C_{12}+C_{23}+C_{31})$, for different weak measurement strengths, considering $C_{12}=\frac{2}{3}$ and $\gamma=0.1$.

optimum value of Svetlichny operator is 4.354, which occurs when $\eta=1$, $C'_{12}=C'_{23}=C'_{31}=2/3$, and $\theta'_a=\theta'_b=\theta'_c=54.736^o$. The violation of Svetlichny inequality with respect to the varying sum of concurrences of three reduced states of ρ_W^{wk} is depicted in Figure 3.23.

Furthermore, Pati and Agrawal [Agrawal and Pati, 2006] have shown that there is a special class of W states, Eq. (3.4), which can be used for deterministic teleportation and dense coding. Considering the importance of such a class in quantum information and computation, we characterize nonlocal properties of these states under noisy conditions. For this, we consider the set of states given in Eq. (3.4) and assume the phase vectors δ and ζ to be 0 for mathematical convenience. The first term $\langle ABC\rangle$ in Eq. (3.6) for the evolved three-qubit state $\rho_{W_n}^{wk}$ can be represented as

$$\begin{aligned}\langle ABC\rangle_{\rho_{W_n}^{wk}} &= \cos\theta_b\left(C''_{31}\sin\theta_a\sin\theta_c\cos\phi_{ac}-\Delta'\cos\theta_a\cos\theta_c\right)\\ &+ \sin\theta_b\left(C''_{12}\cos\theta_a\sin\theta_c\cos\phi_{bc}+C''_{23}\sin\theta_a\cos\theta_c\cos\phi_{ab}\right)\end{aligned} \tag{3.65}$$

where $\Delta'=\frac{(2+\gamma(\eta-1))}{(2-\gamma(\eta-1))}$, $\cos\phi_{ab}=\cos(\phi_a-\phi_b)$, and $C''_{12}=\frac{2\sqrt{n}}{\sqrt{n+1}(2-\gamma(\eta-1))}$, $C''_{23}=\frac{2\sqrt{n}}{(n+1)(2-\gamma(\eta-1))}$, and $C''_{31}=\frac{2}{\sqrt{n+1}(2-\gamma(\eta-1))}$ are the concurrences of bipartite states associated with finally shared state $\rho_{W_n}^{wk}$. The optimized value of Svetlichny operator for the state $\rho_{W_n}^{wk}$ can be calculated in a similar fashion as in the case of ρ_W^{wk}, and can be given as

$$S_v\left(\rho_{W_n}^{wk}\right)_{opt}=4\left(s_1\Delta'+s_2C''_{12}+s_3C''_{23}+s_4C''_{31}\right) \tag{3.66}$$

The violation of Svetlichny inequality for W_n class states is confirmed, when $(s_1\Delta'+s_2C''_{12}+s_3C''_{23}+s_4C''_{31})>1$. Figure 3.24 and Figure 3.25 describe the effects of weak measurement strength η, considering $\gamma=0.1$, on the optimum value of the Svetlichny operator against the varying sum of concurrences of the three reduced bipartite states of $\rho_{W_n}^{wk}$ and the state parameter n for W_n states, respectively.

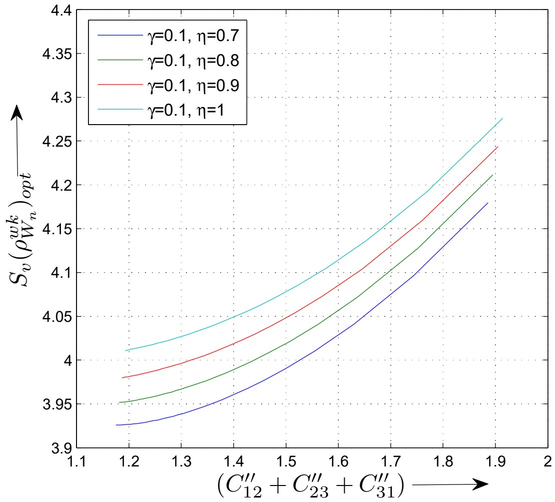

Figure 3.24 : $S_v(\rho^{wk}_{W_n})_{opt}$ with respect to the varying sum of concurrences $(C''_{12}+C''_{23}+C''_{31})$, for different weak measurement strengths, considering $\gamma = 0.1$.

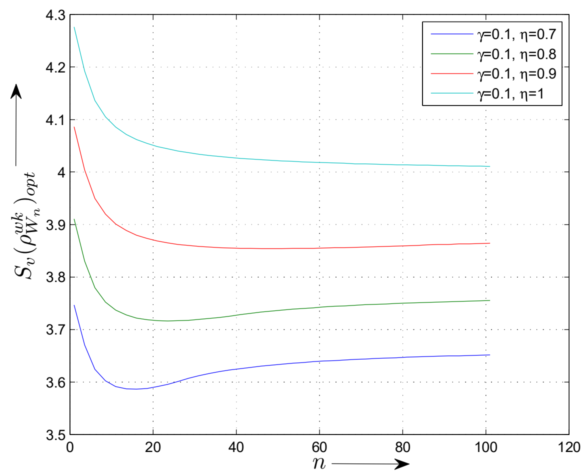

Figure 3.25 : Maximum expectation value of $S_v(\rho^{wk}_{W_n})_{opt}$ vs n for W_n type states at different weak measurement strengths, considering $\gamma = 0.1$.

3.6 NONLOCALITY IN THE FOUR-QUBIT GHZ STATES

The Svetlichny inequality for a four-qubit system can be expressed as

$$S'_v(\rho) \equiv \left|\langle\psi| S'_v |\psi\rangle\right| \leq 8 \tag{3.67}$$

Here the Svetlichny operator S'_v is given by

$$S'_v = (AB - A'B')K + (AB' + A'B)K' \tag{3.68}$$

where $K = C(D-D') - C'(D+D')$, $K' = C'(D'-D) - C(D+D')$, and measurement operators are defined in a similar fashion as for three-qubit systems. The violation of Svetlichny inequality in

Eq. (3.67) confirms the presence of nonlocal correlations in an underlying state. In this section, we analyse the effect of decoherence and weak measurements on nonlocality of the generalized four-qubit GHZ states, i.e.,

$$|\Psi_G\rangle = \cos\theta\,|0000\rangle + \sin\theta\,|1111\rangle \tag{3.69}$$

For this, we first establish an analytical relation between nonlocality of the finally shared state with four-qubit entanglement measure of the initial state $|\Psi_G\rangle$, state parameter, noise parameter, and the weak measurement strength. We further demonstrate the relation between nonlocality of the evolved mixed state with the negativity of the finally shared state as an entanglement measure.

In order to analyse the effect of decoherence and weak measurements, we now consider a scenario where Alice prepares a four-qubit pure GHZ state $|\Psi_G\rangle$, performs weak measurement on qubits 2, 3 and 4 and then sends second qubit to Bob, third to Charlie, and fourth to Dave through amplitude-damping channels. After receiving the qubits, Bob, Charlie and Dave perform reverse quantum measurements on their respective qubits. For simplicity, we again consider identical decoherence parameters and identical weak measurement strengths for every channel. Therefore, the expectation value $\langle ABCD\rangle$ in Eq. (3.68) with respect to the finally shared state ρ_G^{wk} is

$$\langle ABCD\rangle_{\rho_G^{wk}} = \frac{1}{N_A''}\left[\kappa\cos\theta_a\cos\theta_b\cos\theta_c\cos\theta_d + \sin 2\theta\cos\phi_{abcd}\sin\theta_a\sin\theta_b\sin\theta_c\sin\theta_d\right] \tag{3.70}$$

where $\kappa = \left(\cos^2\theta + (1+\gamma(\eta-1))^3\sin^2\theta\right)$, $N_A'' = \left(\cos^2\theta + (1+\gamma(1-\eta))^3\sin^2\theta\right)$ and $\phi_{abcd} = (\phi_a+\phi_b+\phi_c+\phi_d)$. Similarly, one can evaluate other terms in Eq. (3.68), and rearrange it as a sum of two terms so that

$$S_v'\left(\rho_G^{wk}\right) = \frac{1}{N_A''}|\kappa t_1 + \sin 2\theta t_2| \tag{3.71}$$

Here t_1 and t_2 are defined as

$$t_1 = \cos\theta_a\cos\theta_b G_Q + \cos\theta_a\cos\theta_{b'}G_{Q'} + \cos\theta_{a'}\cos\theta_b G_{Q'} - \cos\theta_{a'}\cos\theta_{b'}G_Q \tag{3.72}$$

$$t_2 = \sin\theta_a\sin\theta_b f_{ab} + \sin\theta_a\sin\theta_{b'}f_{ab'} + \sin\theta_{a'}\sin\theta_b f_{a'b} - \sin\theta_{a'}\sin\theta_{b'}f_{a'b'} \tag{3.73}$$

where

$$G_Q = \cos\theta_c(\cos\theta_d - \cos\theta_{d'}) - \cos\theta_{c'}(\cos\theta_d + \cos\theta_{d'}) \tag{3.74}$$

$$G_{Q'} = \cos\theta_{c'}(\cos\theta_{d'} - \cos\theta_d) - \cos\theta_c(\cos\theta_d + \cos\theta_{d'}) \tag{3.75}$$

and

$$\begin{aligned} f_{ab} &= \sin\theta_c(\sin\theta_d\cos\phi_{abcd} - \sin\theta_{d'}\cos\phi_{abcd'}) \\ &- \sin\theta_{c'}(\sin\theta_d\cos\phi_{abc'd} + \sin\theta_{d'}\cos\phi_{abc'd'}) \end{aligned} \tag{3.76}$$

$$\begin{aligned} f_{ab'} &= \sin\theta_{c'}(\sin\theta_{d'}\cos\phi_{ab'c'd'} - \sin\theta_d\cos\phi_{ab'c'd}) \\ &- \sin\theta_c(\sin\theta_d\cos\phi_{ab'cd} + \sin\theta_{d'}\cos\phi_{ab'cd'}) \end{aligned} \tag{3.77}$$

$$\begin{aligned} f_{a'b} &= \sin\theta_{c'}(\sin\theta_{d'}\cos\phi_{a'bc'd'} - \sin\theta_d\cos\phi_{a'bc'd}) \\ &- \sin\theta_c(\sin\theta_d\cos\phi_{a'bcd} + \sin\theta_{d'}\cos\phi_{a'bcd'}) \end{aligned} \tag{3.78}$$

$$\begin{aligned} f_{a'b'} &= \sin\theta_c(\sin\theta_d\cos\phi_{a'b'cd} - \sin\theta_{d'}\cos\phi_{a'b'cd'}) \\ &- \sin\theta_{c'}(\sin\theta_d\cos\phi_{a'b'c'd} + \sin\theta_{d'}\cos\phi_{a'b'c'd'}) \end{aligned} \tag{3.79}$$

For evaluating the relationship between t_1 and t_2, we further consider two unit vectors $\hat{p}$ and $\hat{p}'$ where $\hat{b}+\hat{b}' = 2\hat{p}\cos\theta_1$ and $\hat{b}-\hat{b}' = 2\hat{p}'\sin\theta_1$ such that

$$\hat{p}.\hat{p}' = \cos\theta_p\cos\theta_{p'} + \sin\theta_p\sin\theta_{p'}\cos(\phi_p - \phi_{p'}) = 0 \tag{3.80}$$

Therefore, t_1 and t_2 can be re-expressed as

$$\begin{aligned} |t_1| &= |l_{ap'cd}\sin\theta_1 - l_{apcd'}\cos\theta_1 - l_{apc'd}\cos\theta_1 - l_{ap'c'd'}\sin\theta_1 \\ &+ l_{a'pc'd'}\cos\theta_1 - l_{a'p'c'd}\sin\theta_1 - l_{a'pcd}\cos\theta_1 - l_{a'p'cd'}\sin\theta_1| \end{aligned} \tag{3.81}$$

and

$$\begin{aligned} |t_2| &= |s_{ap'cd}\sin\theta_1 - s_{apcd'}\cos\theta_1 - s_{apc'd}\cos\theta_1 - s_{ap'c'd'}\sin\theta_1 \\ &+ s_{a'pc'd'}\cos\theta_1 - s_{a'p'c'd}\sin\theta_1 - s_{a'pcd}\cos\theta_1 - s_{a'p'cd'}\sin\theta_1| \end{aligned} \tag{3.82}$$

where

$$l_{ap'cd} = 2\cos\theta_a\cos\theta_{p'}\cos\theta_c\cos\theta_d \tag{3.83}$$
$$s_{ap'cd} = 2\sin\theta_a\sin\theta_{p'}\sin\theta_c\sin\theta_d\cos\phi_{ap'cd} \tag{3.84}$$

The other coefficients $l_{apcd'}$, $s_{apcd'}$ *etc.* can be defined in a similar fashion with primes on different angles. In order to simplify and optimize the expressions further, we assume $\theta_c = \theta_{c'}$, and define two unit vectors $\hat{q}$ and $\hat{q}'$ such that $\hat{d}+\hat{d}' = 2\vec{q}\cos\theta_2$ and $\hat{d}-\hat{d}' = 2\vec{q}'\sin\theta_2$, i.e.,

$$\hat{q}.\hat{q}' = \cos\theta_q\cos\theta_{q'} + \sin\theta_q\sin\theta_{q'}\cos(\phi_q - \phi_{q'}) = 0 \tag{3.85}$$

This allows us to re-express Eq. (3.81) and Eq. (3.82) as

$$|t_1| = |l'_{ap'cq'}\sin\theta_1\sin\theta_2 - l'_{apcq}\cos\theta_1\cos\theta_2 - l'_{a'pcq'}\cos\theta_1\sin\theta_2 - l'_{a'p'cq}\sin\theta_1\cos\theta_2| \tag{3.86}$$

and

$$|t_2| = |s'_{ap'cq'}\sin\theta_1\sin\theta_2 - s'_{apcq}\cos\theta_1\cos\theta_2 - s'_{a'pcq'}\cos\theta_1\sin\theta_2 - s'_{a'p'cq}\sin\theta_1\cos\theta_2| \tag{3.87}$$

where

$$l'_{apcq} = 4\cos\theta_a\cos\theta_p\cos\theta_c\cos\theta_q \tag{3.88}$$
$$s'_{apcq} = 4\sin\theta_a\sin\theta_p\sin\theta_c\sin\theta_q\cos\phi_{apcq} \tag{3.89}$$

From Eq. (3.86) and Eq. (3.87), one can get

$$\begin{aligned} |t_1| &\leq |l'_{ap'cq'}||\sin\theta_1||\sin\theta_2| + |l'_{apcq}||\cos\theta_1||\cos\theta_2| \\ &+ |l'_{a'pcq'}||\cos\theta_1||\sin\theta_2| + |l'_{a'p'cq}||\sin\theta_1||\cos\theta_2| \end{aligned} \tag{3.90}$$
$$\begin{aligned} |t_2| &\leq |s'_{ap'cq'}||\sin\theta_1||\sin\theta_2| + |s'_{apcq}||\cos\theta_1||\cos\theta_2| \\ &+ |s'_{a'pcq'}||\cos\theta_1||\sin\theta_2| + |s'_{a'p'cq}||\sin\theta_1||\cos\theta_2| \end{aligned} \tag{3.91}$$

Using these inequalities,the iterative maximization of Eq. (3.71) can be summarized below as

$$\begin{aligned}
2\sqrt{2}\kappa|t_1|+|t_2| &\leq \Big[\Big\{(2\sqrt{2}\kappa|l'_{apcq}|+|s'_{apcq}|)|\cos\theta_1|+(2\sqrt{2}\kappa|l'_{a'p'cq}|+|s'_{a'p'cq}|)|\sin\theta_1|\Big\}|\cos\theta_2| \\
&+ \Big\{(2\sqrt{2}\kappa|l'_{a'pcq'}|+|s'_{a'pcq'}|)|\cos\theta_1|+(2\sqrt{2}\kappa|l'_{ap'cq'}|+|s'_{ap'cq'}|)|\sin\theta_1|\Big\}|\sin\theta_2|\Big] \qquad (3.92)\\
2\sqrt{2}\kappa|t_1|+|t_2| &\leq \Big[\Big\{(2\sqrt{2}\kappa|l'_{apcq}|+|s'_{apcq}|)|\cos\theta_1|+(2\sqrt{2}\kappa|l'_{a'p'cq}|+|s'_{a'p'cq}|)|\sin\theta_1|\Big\}^2 \\
&+ \Big\{(2\sqrt{2}\kappa|l'_{a'pcq'}|+|s'_{a'pcq'}|)|\cos\theta_1|+(2\sqrt{2}\kappa|l'_{ap'cq'}|+|s'_{ap'cq'}|)|\sin\theta_1|\Big\}^2\Big]^{\frac{1}{2}} \qquad (3.93)\\
2\sqrt{2}\kappa|t_1|+|t_2| &\leq \Big[(2\sqrt{2}\kappa|l'_{apcq}|+|s'_{apcq}|)^2+(2\sqrt{2}\kappa|l'_{a'p'cq}|+|s'_{a'p'cq}|)^2 \\
&+ (2\sqrt{2}\kappa|l'_{a'pcq'}|+|s'_{a'pcq'}|)^2+(2\sqrt{2}\kappa|l'_{ap'cq'}|+|s'_{ap'cq'}|)^2\Big]^{\frac{1}{2}} \qquad (3.94)
\end{aligned}$$

where Eq. (3.92) is maximized with respect to θ_2, and the first and second terms in the Eq. (3.93) are maximized separately with respect to θ_1. To simplify and optimize Eq. (3.94), we use Eq. (3.88) and Eq. (3.89), such that

$$(2\sqrt{2}\kappa|l'_{apcq}|+|s'_{apcq}|)=8\sqrt{2}\kappa|\cos\theta_a\cos\theta_p\cos\theta_c\cos\theta_q|+4|\sin\theta_a\sin\theta_p\sin\theta_c\sin\theta_q\cos\phi_{apcq}| \qquad (3.95)$$

Eq. (3.95) when maximized with respect to θ_a, using the inequality (3.12), gives

$$(2\sqrt{2}\kappa|l'_{apcq}|+|s'_{apcq}|)\leq 4\left[8\kappa^2\cos^2\theta_c\cos^2\theta_p\cos^2\theta_q+\sin^2\theta_c\sin^2\theta_p\sin^2\theta_q\cos^2\phi_{apcq}\right]^{\frac{1}{2}} \qquad (3.96)$$

Similarly, the other terms in Eq. (3.94) can be evaluated as

$$\begin{aligned}
(2\sqrt{2}\kappa|l'_{ap'cq'}|+|s'_{ap'cq'}|) &\leq 4\left[8\kappa^2\cos^2\theta_c\cos^2\theta_{p'}\cos^2\theta_{q'}+\sin^2\theta_c\sin^2\theta_{p'}\sin^2\theta_{q'}\cos^2\phi_{ap'cq'}\right]^{\frac{1}{2}} \qquad (3.97)\\
(2\sqrt{2}\kappa|l'_{a'p'cq}|+|s'_{a'p'cq}|) &\leq 4\left[8\kappa^2\cos^2\theta_c\cos^2\theta_{p'}\cos^2\theta_q+\sin^2\theta_c\sin^2\theta_{p'}\sin^2\theta_q\cos^2\phi_{a'p'cq}\right]^{\frac{1}{2}} \qquad (3.98)\\
(2\sqrt{2}\kappa|l'_{a'pcq'}|+|s'_{a'pcq'}|) &\leq 4\left[8\kappa^2\cos^2\theta_c\cos^2\theta_p\cos^2\theta_{q'}+\sin^2\theta_c\sin^2\theta_p\sin^2\theta_{q'}\cos^2\phi_{a'pcq'}\right]^{\frac{1}{2}} \qquad (3.99)
\end{aligned}$$

where, for optimization, we consider $\cos^2\phi_{apcq}=\cos^2\phi_{ap'cq'}=\cos^2\phi_{a'p'cq}=\cos^2\phi_{a'pcq'}=1$. Therefore, using Eqs. (3.96-3.99); Eq. (3.94) can be re-expressed as

$$\begin{aligned}
2\sqrt{2}\kappa|t_2|+|t_1| &\leq 4\left[8\kappa^2\cos^2\theta_c\cos^2\theta_q\left(\cos^2\theta_p+\cos^2\theta_{p'}\right)+\sin^2\theta_c\sin^2\theta_q\left(\sin^2\theta_p+\sin^2\theta_{p'}\right)\right.\\
&+ \left.8\kappa^2\cos^2\theta_c\cos^2\theta_{q'}\left(\cos^2\theta_p+\cos^2\theta_{p'}\right)+\sin^2\theta_c\sin^2\theta_{q'}\left(\sin^2\theta_p+\sin^2\theta_{p'}\right)\right]^{\frac{1}{2}} \qquad (3.100)
\end{aligned}$$

Considering the orthogonality of unit vectors $\hat{p}$ and $\hat{p}'$, the maximum value of $(\sin^2\theta_p+\sin^2\theta_{p'})$ is 2 and maximum value of $(\cos^2\theta_p+\cos^2\theta_{p'})$ is 1, i.e.,

$$2\sqrt{2}\kappa|t_1|+|t_2|\leq 4\left[8\kappa^2\cos^2\theta_c(\cos^2\theta_q+\cos^2\theta_{q'})+2\sin^2\theta_c(\sin^2\theta_q+\sin^2\theta_{q'})\right]^{\frac{1}{2}} \qquad (3.101)$$

Similarly, from the orthogonality of unit vectors $\hat{q}$ and $\hat{q}'$, Eq. (3.101) can be further optimized as

$$2\sqrt{2}\kappa|t_1| + |t_2| \leq 4\left[8\kappa^2\cos^2\theta_c + 4\sin^2\theta_c\right]^{\frac{1}{2}} \tag{3.102}$$

A further maximization on the parameter κ gives

$$2\sqrt{2}|t_1| + |t_2| \leq 8\left[1+\cos^2\theta_c\right]^{\frac{1}{2}} \leq 8\sqrt{2} \tag{3.103}$$

Therefore, the relationship between t_1 and t_2 can be defined as

$$|t_2| \leq 8\sqrt{2} - 2\sqrt{2}|t_1| \tag{3.104}$$

Using Eq. (3.104), the optimum value of Svetlichny operator in Eq. (3.71) can now be given as

$$S'_v\left(\rho_G^{wk}\right)_{opt} \leq \frac{1}{N''_A}\left[8\sqrt{2}\sin 2\theta + (\kappa - 2\sqrt{2}\sin 2\theta)|t_1|\right] \tag{3.105}$$

Clearly, for states lying in the range

$$(\kappa - 2\sqrt{2}\sin 2\theta) \geq 0, \tag{3.106}$$

the bound of Svetlichny operator in Eq. (3.105) is maximized when t_1 attains its maximum value of 4, and hence the corresponding value of $|t_2| = 0$. Therefore, the expression for the maximum value of Svetlichny operator for the states in range given by Eq. (3.106) is

$$S'_v\left(\rho_G^{wk}\right)_{opt} = \frac{4\kappa}{N''_A} \tag{3.107}$$

Similarly, for the states lying in the range

$$(\kappa - 2\sqrt{2}\sin 2\theta) \leq 0 \tag{3.108}$$

the bound of Svetlichny operator is maximized when $|t_1| = 0$, and $|t_2|$ is $8\sqrt{2}$. Therefore, the expression for maximum value of Svetlichny operator for the states satisfying Eq. (3.108) is

$$S'_v\left(\rho_G^{wk}\right)_{opt} = \frac{1}{N''_A}\left[8\sqrt{2}\sin 2\theta\right] \tag{3.109}$$

Hence, the optimum expectation value of the Svetlichny operator for finally shared state is now given by

$$S'_v\left(\rho_G^{wk}\right)_{opt} \leq \begin{cases} \frac{4\kappa}{N''_A}, & 2\sqrt{2}\sin 2\theta \leq \kappa \\ \frac{8}{N''_A}\sqrt{2\sin^2 2\theta}, & 2\sqrt{2}\sin 2\theta \geq \kappa \end{cases} \tag{3.110}$$

Eq. (3.110) can be re-expressed in form of the four-qubit entanglement of the initially shared generalized GHZ state, given by $\tau_4 = \sin^2 2\theta$, such that

$$S'_v\left(\rho_G^{wk}\right)_{opt} \leq \begin{cases} \frac{4\kappa}{N''_A}, & \tau_4 \leq \frac{\kappa}{8} \\ \frac{8}{N''_A}\sqrt{2\tau_4}, & \tau_4 \geq \frac{\kappa}{8} \end{cases} \tag{3.111}$$

For perfect channels, i.e., with no noise or amplitude-damping ($\gamma = 0$), one can deduce that the maximum expectation value of Svetlichny operator is

$$S'_v\left(\rho_G^{wk}\right) \leq \begin{cases} 4, & \tau_4 \leq \frac{1}{8} \\ 8\sqrt{2\tau_4}, & \tau_4 \geq \frac{1}{8} \end{cases} \tag{3.112}$$

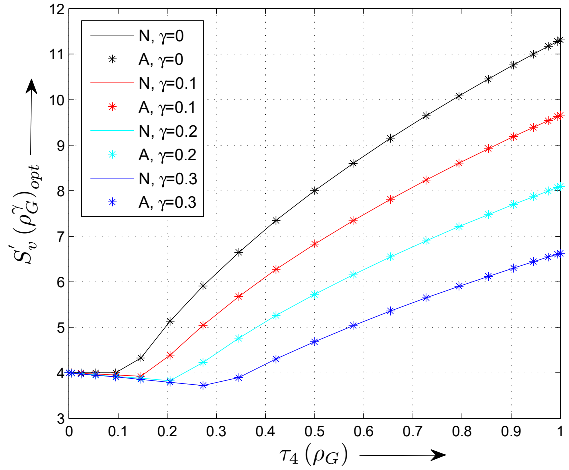

Figure 3.26 : Estimation of $S'_v(\rho_G^{\gamma})_{opt}$ with respect to 4-qubit entanglement (τ_4) of the initial GHZ state considering four different values of decoherence parameter γ.

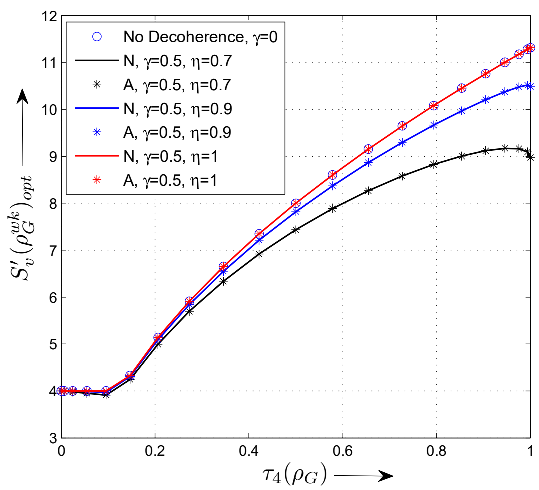

Figure 3.27 : Estimation of $S'_v(\rho_G^{wk})_{opt}$ with respect to 4-qubit entanglement (τ_4) of the initial GHZ state for different weak measurement strengths, considering $\gamma = 0.5$.

Similarly, the effect of amplitude-damping channel completely vanishes when $\eta = 1$, i.e., the finally shared state becomes a pure four-qubit state . Therefore, the expression for optimized expectation value of Svetlichny operator will be the same as in Eq. (3.112). Based on our results, in Figure 3.26, we demonstrate the effect of noise parameter γ on the expectation value of Svetlichny operator against entanglement of the initially shared four-qubit GGHZ state. Similarly, Figure 3.27 demonstrates the effect of weak measurement strength η on the expectation value of Svetlichny operator against entanglement of the initially shared four-qubit GGHZ state, considering noise parameter $\gamma = 0.5$. Clearly, performing weak measurements on the qubits strengthens the degree of correlation in the finally shared state. The analytical result obtained here completely agrees with the numerical result obtained for the violation of Svetlichny inequality. For a maximally

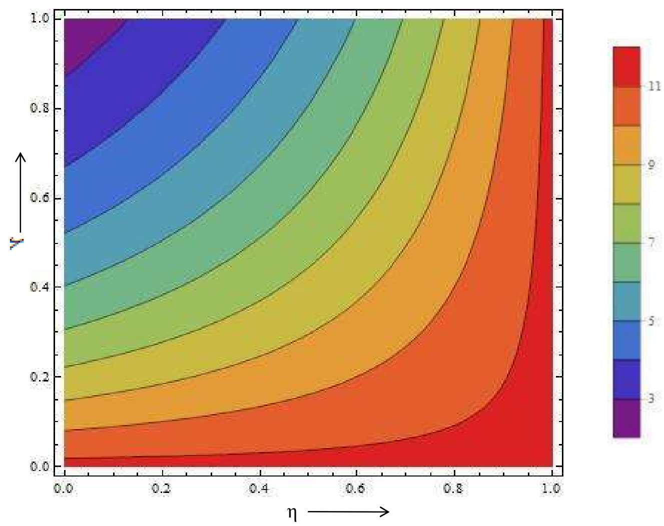

Figure 3.28 : Maximum expectation value of the Svetlichny operator as a function of noise parameter γ for the finally shared state at different values of weak measurement strength.

entangled initial state, Figure 3.28 describes the effects of noise parameter γ and weak measurement strength η on the maximum expectation value of Svetlichny operator. Therefore, the use of weak measurement and quantum measurement reversal protects genuine four-qubit nonlocality.

In the absence of weak measurement and its reversal operations, i.e., if the system is only subjected to an amplitude-damping noise then the expectation value of $\langle ABCD \rangle$ (Eq. (3.68)) with respect to finally shared state ρ_G^γ can be given as

$$\langle ABCD \rangle_{\rho_G^\gamma} = \left[\kappa' \cos\theta_a \cos\theta_b \cos\theta_c \cos\theta_d + (1-\gamma)^{3/2} \sin 2\theta \cos\phi_{abcd} \sin\theta_a \sin\theta_b \sin\theta_c \sin\theta_d\right] \tag{3.113}$$

where $\kappa' = \left(\cos^2\theta + (1-2\gamma)^3 \sin^2\theta\right)$, and $\phi_{abcd} = (\phi_a + \phi_b + \phi_c + \phi_d)$. Therefore, the optimum expectation value of Svetlichny operator for finally shared state in this scenario can be evaluated as

$$S'_v\left(\rho_G^\gamma\right)_{opt} = \begin{cases} 4\left(\cos^2\theta + (1-2\gamma)^3 \sin^2\theta\right) & \left(2(1-\gamma)^{3/2}\sqrt{2}\sin 2\theta\right) \leq \kappa' \\ 8\sqrt{2(1-\gamma)^3 \sin^2 2\theta}, & \left(2(1-\gamma)^{3/2}\sqrt{2}\sin 2\theta\right) \geq \kappa' \end{cases} \tag{3.114}$$

Similar to the three-qubit GGHZ case, we further evaluate a numerical relation between the maximum expectation value of Svetlichny operator and negativity of finally shared mixed state. The effect of amplitude-damping channel and weak measurement on the negativity of finally shared state is depicted in Figure 3.29 and Figure 3.30, respectively. Figure 3.31 demonstrates the variation of maximum expectation value of Svetlichny operator vs negativity for different values of weak measurement strength, considering the noise parameter $\gamma = 0.5$.

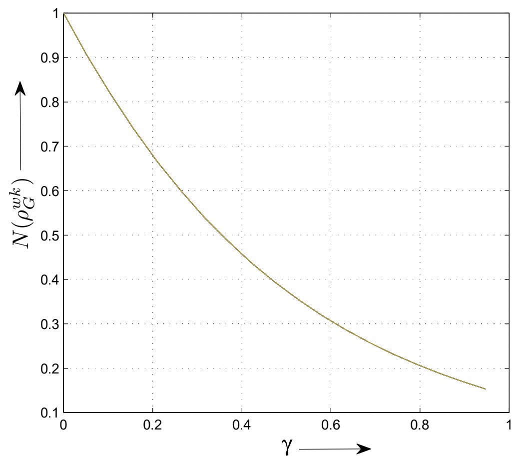

Figure 3.29 : Negativity of the finally shared 4-qubit state as a function of noise parameter γ .

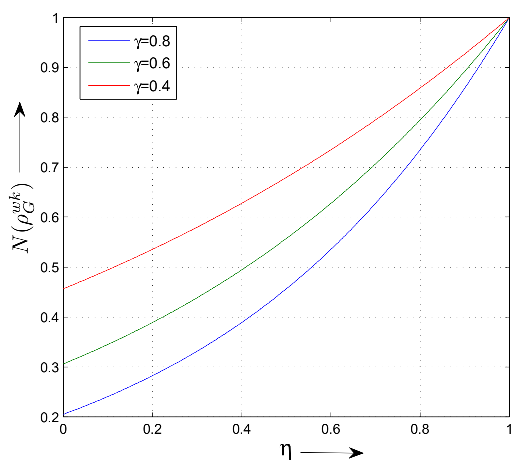

Figure 3.30 : Negativity of the finally shared 4-qubit state as a function of weak measurement strength at three different values of noise parameter γ.

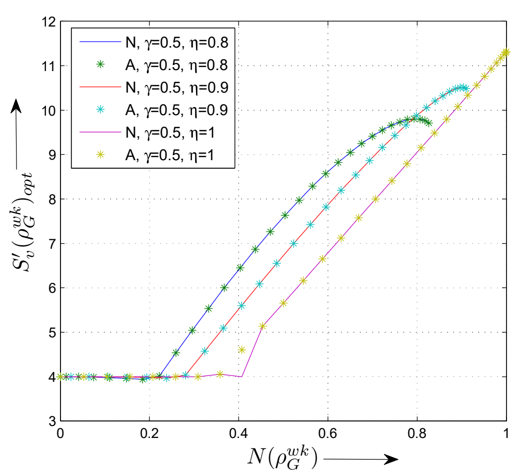

Figure 3.31 : Estimation of $S'_v(\rho_G^{wk})_{opt}$ with respect to Negativity $N(\rho_G^{wk})$ for different values of weak measurement strengths, considering $\gamma = 0.5$.

3.7 SUMMARY

To summarise, we have analysed the effect of decoherence using amplitude-damping channels and weak measurement and its reversal operations on genuine three- and four-qubit nonlocality. We have also analysed the effect of phase-damping and depolarizing channels under the applications of weak measurement and its reversal operations on genuine three-qubit nonlocality. Our analysis for generalized three- and four-qubit GHZ states, three-qubit W class and W_n states allowed us to characterize the multiqubit nonlocal correlations in terms of noise parameters and strengths of weak measurements. The results obtained here clearly suggest that the effect of amplitude-damping on multiqubit nonlocality can be reduced or completely removed depending on the strengths of weak measurement and its reversal operations. We have further shown that the analytical results obtained in all the cases are in excellent agreement with the numerical results. In future, it will be interesting to investigate the usefulness of finally shared three-qubit and four-qubit mixed states for quantum information and computation.

…